



HAL
open science

Cell-to-cell spread of vaccinia virus is promoted by TGF - β -independent Smad4 signalling

Anjali Gowripalan, Caitlin R Abbott, Christopher Mckenzie, Weng S Chan,
Gunasegaran Karupiah, Laurence Levy, Timothy P Newsome

► To cite this version:

Anjali Gowripalan, Caitlin R Abbott, Christopher Mckenzie, Weng S Chan, Gunasegaran Karupiah, et al.. Cell-to-cell spread of vaccinia virus is promoted by TGF - β -independent Smad4 signalling. Cellular Microbiology, 2020, 22, 10.1111/cmi.13206 . hal-04031971

HAL Id: hal-04031971

<https://hal.sorbonne-universite.fr/hal-04031971v1>

Submitted on 16 Mar 2023


HAL is a multi-disciplinary open access archive for the deposit and dissemination of scientific research documents, whether they are published or not. The documents may come from teaching and research institutions in France or abroad, or from public or private research centers.

L'archive ouverte pluridisciplinaire **HAL**, est destinée au dépôt et à la diffusion de documents scientifiques de niveau recherche, publiés ou non, émanant des établissements d'enseignement et de recherche français ou étrangers, des laboratoires publics ou privés.

RESEARCH ARTICLE

WILEY

Cell-to-cell spread of vaccinia virus is promoted by TGF- β -independent Smad4 signalling

Anjali Gowripalan¹ | Caitlin R. Abbott¹ | Christopher McKenzie¹ |
Weng S. Chan¹ | Gunasegaran Karupiah³ | Laurence Levy² | Timothy P. Newsome¹ 

¹School of Life and Environmental Sciences,
The University of Sydney, Sydney, New South
Wales, Australia

²Sorbonne Université, Inserm, Centre de
Recherche Saint-Antoine, CRSA, Paris, France

³Tasmanian School of Medicine, The
University of Tasmania, Hobart, Tasmania,
Australia

Correspondence

Timothy P. Newsome, School of Life and
Environmental Science, Life, Earth and
Environmental Sciences Building F22, The
University of Sydney, 2006, Sydney, Australia.
Email: tim.newsome@sydney.edu.au

Funding information

National Health and Medical Research Council,
Grant/Award Number: 632785

Abstract

The induction of Smad signalling by the extracellular ligand TGF- β promotes tissue plasticity and cell migration in developmental and pathological contexts. Here, we show that vaccinia virus (VACV) stimulates the activity of Smad transcription factors and expression of TGF- β /Smad-responsive genes at the transcript and protein levels. Accordingly, infected cells share characteristics to those undergoing TGF- β /Smad-mediated epithelial-to-mesenchymal transition (EMT). Depletion of the Smad4 protein, a common mediator of TGF- β signalling, results in an attenuation of viral cell-to-cell spread and reduced motility of infected cells. VACV induction of TGF- β /Smad-responsive gene expression does not require the TGF- β ligand or type I and type II TGF- β receptors, suggesting a novel, non-canonical Smad signalling pathway. Additionally, the spread of ectromelia virus, a related orthopoxvirus that does not activate a TGF- β /Smad response, is enhanced by the addition of exogenous TGF- β . Together, our results indicate that VACV orchestrates a TGF- β -like response via a unique activation mechanism to enhance cell migration and promote virus spread.

KEYWORDS

cell migration, PAI-1, Smad4, TGF- β , vaccinia virus

1 | INTRODUCTION

The *Orthopox* genus contains many notable viruses, including the infamous human pathogen variola virus, the causative agent of smallpox; ectromelia virus (ECTV), the causative agent of mousepox; and vaccinia virus (VACV), the live vaccine used to successfully eradicate smallpox (Fenner, 1993). Much of our understanding of the orthopoxvirus infection cycle derives from studies with VACV. Initially, virions infect susceptible host cells via a fusion mechanism (for mature virus) or a combination of fusogenic and non-fusogenic mechanisms (for wrapped virus) (Doms, Blumenthal, & Moss, 1990; Law, Carter, Roberts, Hollinshead, & Smith, 2006; Mercer & Helenius, 2008; Schmidt, Bleck, Helenius, & Mercer, 2011). Following entry, viral cores are delivered to

the cytoplasm and a replication centre is established at a perinuclear site (Condit, Moussatche, & Traktman, 2006; Liu, Cooper, Howley, & Hayball, 2014). These early stages of virus replication are dominated by efforts to subdue host defences triggered by viral challenge (Bidgood & Mercer, 2015). For instance, prior to viral gene expression, virion-derived proteins released from lateral bodies act directly to suppress antiviral responses, such as those mediated by STAT1 (Schmidt et al., 2013). Products of early gene expression then degrade host mRNAs (Parrish, Resch, & Moss, 2007), inhibit the cytoplasmic DNA sensor DNA-dependent protein kinase (Peters et al., 2013) and suppress innate and adaptive immunity (Strnadova et al., 2015; Stuart, Sumner, Lu, Snowden, & Smith, 2016). In the event of a productive infection cycle, viral factors wrest control of major host functions leading to global inhibition of cellular transcription networks (Moss, 1968; Rice & Roberts, 1983). While viral suppression of the host anti-viral response has been well documented, less is known regarding the

Anjali Gowripalan, Caitlin R. Abbott, and Christopher McKenzie contributed equally to this work.

induction of cellular gene expression cascades that promote an environment conducive to virus replication (Bourquain, Dabrowski, & Nitsche, 2013; Rubins, Hensley, Relman, & Brown, 2011).

Complex morphological processes, such as the restructuring of the cell cytoskeleton or the induction of cell motility, are modulated by host cell-signalling pathways in a variety of developmental and pathological contexts (Lamouille, Xu, & Derynck, 2014). One point of focus in tissue plasticity regulation is epithelial-to-mesenchymal transition (EMT) – a phenomenon that results in the dissolution of cell-to-cell junctions, alterations to matrix adhesion, the formation of spindle-shaped cells and increased migratory capacity (Xu, Lamouille, & Derynck, 2009). Prominent EMT-associated signalling pathways are activated by TGF- β , EGF, PDGF, Wnt and Notch, which are associated with gastrulation, neural crest formation, wound healing, cancer metastasis and fibrosis (Lamouille et al., 2014). However, a number of microbes are also able to modulate these pathways to promote pathogenesis and enhance spread in a whole organism. For instance, the induction of EMT is critical during the pathogenesis of *Helicobacter pylori*, which affects the translocation of the scaffold protein CagA to target cells, thereby promoting the destruction of the gastric epithelial barrier (Hatakeyama, 2008). Virus-associated EMT, by way of TGF- β signalling, has also been observed during infection with hepatitis B virus (HBV), Epstein–Barr virus, SARS-associated coronavirus and ebolavirus; and typically correlates with increased production of TGF- β (Cayrol & Flemington, 1995; Kindrachuk et al., 2014; Yoo et al., 1996; Zhao, Nicholls, & Chen, 2008). The potential importance of this phenotype is further evidenced by the presence of TGF- β homologues in the genomes of *Chordopoxvirinae* subfamily members (Afonso et al., 2000; Afonso et al., 2005). Many of the cellular hallmarks that are characteristic of EMT and activated TGF- β signalling are observed during VACV infection yet, until now, a relationship between these has not been investigated. Furthermore, a VACV protein, vaccinia growth factor (VGF), is homologous to a known TGF- β pathway influencer, EGF, and is involved in enhancing infected cell migration (Beerli et al., 2019; Brown, Twardzik, Marquardt, & Todaro, 1985; Wrighton, Lin, & Feng, 2009). Wnt signalling induced by A49 has also recently been observed during VACV infection but the role currently remains unclear (Maluquer de Motes & Smith, 2017).

To investigate novel mechanisms that facilitate the spread of VACV, we characterised the activity of the TGF- β signalling pathway in infected cells. The canonical cellular response to TGF- β is mediated by its binding to the heterotetrameric receptor complex of TGF- β receptor type I (TGFBR1) and TGF- β receptor type II (TGFBR2) proteins (Chaikuad & Bullock, 2016). This leads to the phosphorylation of receptor-regulated Smads (R-Smads), Smad2 and Smad3, and the generation of a binding site for the common Smad, Smad4 (Macias, Martin-Malpartida, & Massague, 2015; Xu et al., 2009). Complexes comprising the R-Smads and Smad4 translocate to the nucleus, where they, along with other cofactors, elicit transcriptional changes resulting in the induction or repression of target gene expression (Macias et al., 2015). We determined that VACV infection induces the activity of Smad2, Smad3 and Smad4 transcription factors as

evidenced by reporter assays, RT-qPCR and immunofluorescence analyses. Depletion of Smad4 led to a reduction in TGF- β target gene expression, an attenuation in virus spread in plaque assays, and an accompanying reduction in infected cell motility. In contrast to TGF- β treatment, VACV-induced, Smad-mediated gene expression did not increase the production of TGF- β , or require TGFBR1 or TGFBR2. This is a novel observation as the activity of R-Smads is thought to require TGFBR1-mediated phosphorylation at a C-terminal SSXS motif. Furthermore, we observed that activation of R-Smad signalling was conserved among the VACV strains, but not the related murine orthopoxvirus, ECTV. Plaques formed by ECTV are significantly smaller in comparison to those formed by VACV, yet ECTV spread could be enhanced with the addition of exogenous TGF- β . Our results indicate that VACV activates a non-canonical TGF- β response to promote the cell-to-cell spread of the virus through the induction of cell motility.

2 | RESULTS

2.1 | VACV infection induces changes to cell behaviours and activity of Smad2, Smad3 and Smad4 transcription complexes

Following infection with VACV-Western Reserve strain (VACV-WR), cells such as HeLa, BSC-1 and HaCaT undergo profound morphological changes, including the loss of cell-to-cell adhesion, drastic modification of the actin cytoskeleton and adoption of different cell shapes (Figure 1a, data not shown). In the early stages of plaque formation, infected cells can also be seen to infiltrate regions of uninfected cells—a process predicted to increase the rate of plaque expansion (Figure 1b) (Beerli et al., 2019; Doceul, Hollinshead, van der Linden, & Smith, 2010). To determine if these morphological changes were accompanied by the activation of signalling pathways associated with cell migration, we examined the activity of TGF- β -responsive elements in VACV-infected cells. The ARE-Luc reporter (Smad2-dependent transcription), the SBR₆-Luc (Smad3-dependent transcription) and the CAGA₁₂-Luc reporters (Smad3/4-dependent transcription) are TGF- β -responsive and were found to be activated upon VACV infection (Figure 1c) (Levy & Hill, 2005). CAGA₁₂-Luc activation was evident from 6 hr post-infection (hpi) and followed similar dynamics to TGF- β treatment (Figure 1d). Infection with related VACV strains Lister, Copenhagen and Ankara, also led to the activation of the CAGA₁₂-Luc reporter (Figure 1e). Infection with the attenuated MVA strain did not activate the CAGA₁₂-Luc reporter.

Upon binding of TGF- β to its cognate receptor complex (comprising TGFBR1 and TGFBR2), cytoplasmic Smad2 and Smad3 are phosphorylated by TGFBR1 at two C-terminal serines in an SSXS motif (S465/S467 and S423/S425, respectively) (Wrighton et al., 2009). Phosphorylation of R-Smads allows these proteins to form a variety of complexes with transcriptional cofactors and is paramount to their activity in regulating gene expression (Chacko et al., 2004). Consistent with the activation of TGF- β reporter assays, we observed elevated

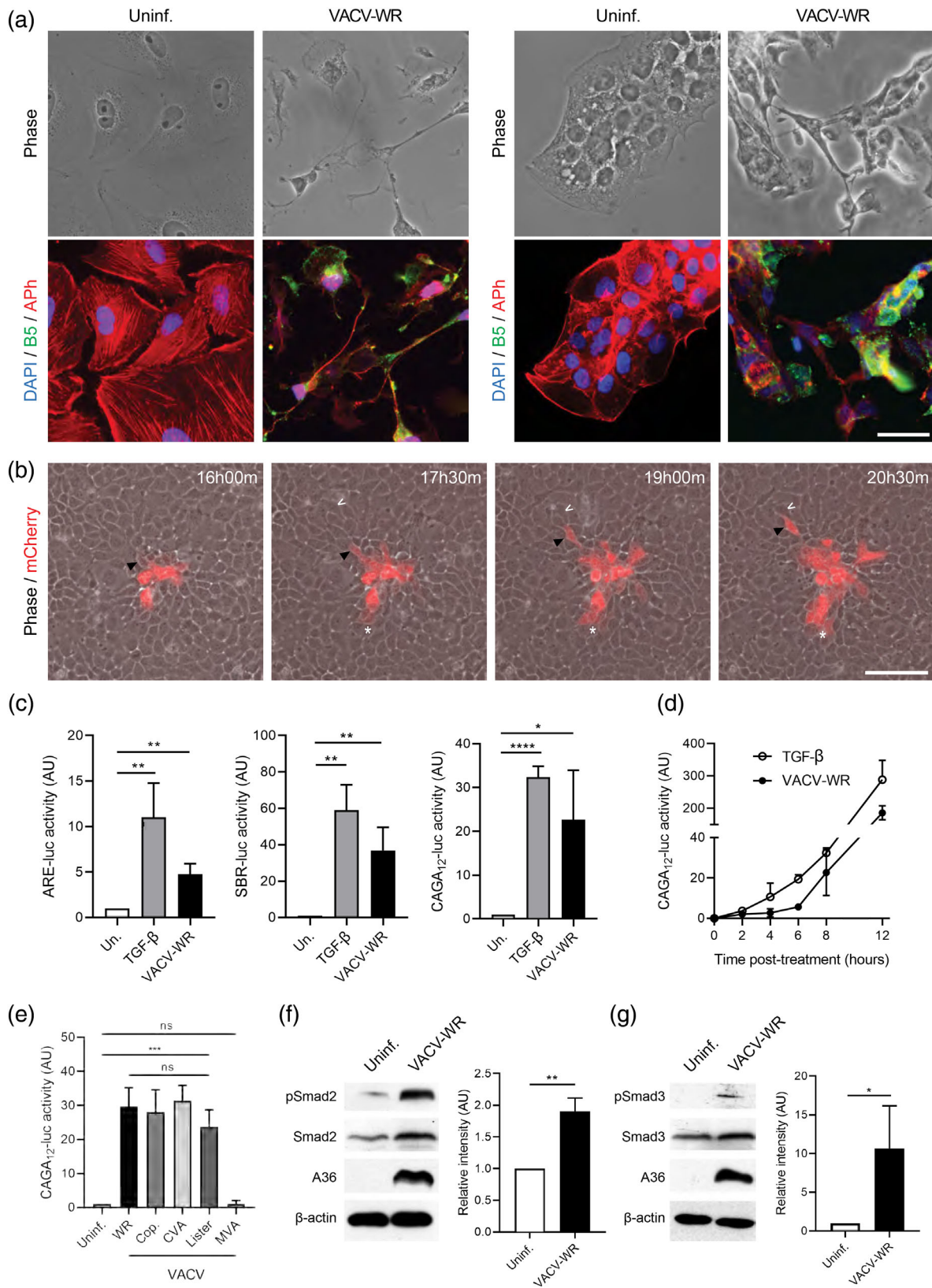


FIGURE 1 Legend on next page.

phosphorylation of Smad2 (S465/S467) (Figure 1f) and Smad3 (S423/S425) (Figure 1g) compared to total Smad2 and Smad3 upon infection, indicating that VACV is capable of activating the first intracellular stage in the canonical TGF- β signalling pathway.

Having established the activity of R-Smad transcriptional complexes in VACV-infected cells at the level of protein phosphorylation and reporter activity, we next sought to determine whether expression of TGF- β -associated target genes was increased upon infection. One Smad3 target, c-JUN, enhances Smad3-mediated signalling through the formation of oncogenic transcription complexes (Zhang, Feng, & Derynck, 1998). Others, such as Snail and Snail2, are key zinc finger transcription factors that mediate EMT in response to TGF- β , Wnt and Notch signalling. The Snail promoter includes binding sites for Smad2, Smad3 and Smad4 (Cho, Baek, Saika, Jeong, & Yoo, 2007; Wang, Shi, Chai, Ying, & Zhou, 2013). Human plasminogen activator inhibitor (PAI-1) protein is a serine protease inhibitor and is induced by TGF- β due to multiple TGF- β -responsive elements in its promoter, which act as binding elements for Smad3/Smad4 complexes (Denkler et al., 1998). We observed the induction of c-JUN, Snail, Snail2 and PAI-1 expression in HaCaT cells infected with VACV (Figure 2a,b). This was evident at both the level of transcription and translation, and conserved in two cell lines commonly used to study EMT and TGF- β signalling; PANC-1 and HT-29 cells (Figure S1a,b). The upregulation of TGF- β -responsive genes upon infection was similar to cells treated with TGF- β , although some differences were observed. PAI-1 induction by VACV-infection, for example, was more pronounced compared to TGF- β treatment in all cell types (Figure 2b). The timing of these responses also varied between conditions; for example, TGF- β treatment induced sustained expression of Snail2 transcripts, while the response to infection with VACV-WR was more transient (Figure 2a). Snail2 was significantly increased in infected cells at 8 hpi ($p = .004$) but subsequently decreased at 10 hpi. Overall, the induction of TGF- β -responsive genes by VACV was observed to be robust, but not identical to TGF- β treatment, in a variety of cells types.

2.2 | Smad4-dependent and Smad4-independent induction of gene expression by TGF- β and VACV

A range of Smad transcriptional complexes with different constituent cofactors are responsible for mediating a TGF- β response. A class of

TGF- β -responsive genes regulated by Smad2 and Smad3 have been shown to be Smad4-dependent, in that they require the common Smad for their induction (Levy & Hill, 2005); for example, PAI-1. To test the Smad4-dependence of TGF- β -responsive genes induced by VACV, we infected HaCaT TRS4 cells that carry a tetracycline (Tet) repressor and Tet-inducible siRNA against Smad4 (Levy & Hill, 2005). Tet-induction of siRNA in TRS4 cells led to a reduction in Smad4 expression but not in matched TR cells that lack the Tet-inducible siRNA (Figure 3a). We then used RT-qPCR to analyse the expression of TGF- β -responsive genes in response to VACV infection under control (no Tet) and Smad4-depleted (Tet-treated) conditions. Consistent with previous studies, we observed that TGF- β treatment of HaCaT cells induced expression of c-JUN and PAI-1, with PAI-1 induction being Smad4 dependent (Figures 3b and S2a) (Levy & Hill, 2005). VACV-infection of HaCaT cells induced c-JUN and PAI-1 expression to a similar extent (Figures 3b and S2a). Viral induction of PAI-1 was also determined to be Smad4-dependent as it was reduced in Tet-treated TRS4 cells, but not TR cells (Figures 3b and S2a). We confirmed by immunofluorescence analysis that induction of Snail and Snail2 was Smad4-independent, and that induction of PAI-1 was Smad4-dependent, both in TGF- β -treated and VACV-infected cells (Figures S2b and 3c). Immunofluorescence analysis of whole VACV plaques confirmed the requirement for Smad4 in the induction of PAI-1 by VACV (Figure 3d). The cell autonomy of virus-induced PAI-1 was evident at the periphery of the VACV plaques (Figure 3e). Taken together, our results indicate that VACV induces expression of c-JUN, Snail, Snail2 and PAI-1, and that as with TGF- β treatment, only the induction of PAI-1 was found to be Smad4-dependent.

2.3 | Loss of Smad4 expression attenuates VACV spread and induced cell motility

We have determined that a component of the TGF- β -response induced by VACV is Smad4-dependent. TRS4 cells, therefore, offer a tractable experimental system to address the role of Smad4 in viral infection and spread. We analysed VACV plaques formed under conditions of Smad4 knockdown, which revealed a 13% reduction in plaque size and altered plaque morphology (Figure 4a,b). The ability of the virus to clear cells within plaques was found to be strongly

FIGURE 1 VACV activates Smad2 and Smad3 signalling. (a) Micrographs of VACV-WR-infected BSC-1 (left) and HaCaT (right) cells at 24 hpi (MOI = 5). Viral protein, B5, nucleic acid (DAPI) and actin (Alexa Phalloidin, Aph) appear green, blue and red respectively. Scale bar = 50 μ m. (b) Live cell imaging of VACV-WR (mCherry)-infected HaCaT cells demonstrating infected cell migration over time. The migration of infected cell (black arrowhead) facilitates the cell-to-cell transmission of virus to more distal cells (white chevron), compared to the infection of adjacent cells in the absence of cell migration (white asterix). Scale bar = 100 μ m. (c) Activity of Smad reporter elements in HaCaT cells following infection with VACV-WR or treatment with TGF- β (* $p < .05$, ** $p < .01$, **** $p < .001$ by unpaired t test). (d) Temporal activation of CAGA₁₂-luc reporter 2-12 hpi with VACV-WR or treatment with TGF- β . (e) Activity of CAGA₁₂-luc reporter 8 hpi with VACV strains Lister, Copenhagen (Cop.), Chorioallantois vaccinia virus Ankara (CVA), and Modified vaccinia Ankara (MVA) (*** $p < .005$ by One-way ANOVA with Tukey's multiple comparisons test). All luciferase data shown as means \pm SD of 3 biological replicates. (f,g) Immunoblot analysis and quantification of (f) Smad2 (S465/S467) and (g) Smad3 (S423/425) phosphorylation in HaCaT cells at 8 hpi with VACV-WR (MOI = 5). Images presented are representative of three independent experiments (* $p < .05$, ** $p < .005$ by unpaired t test)

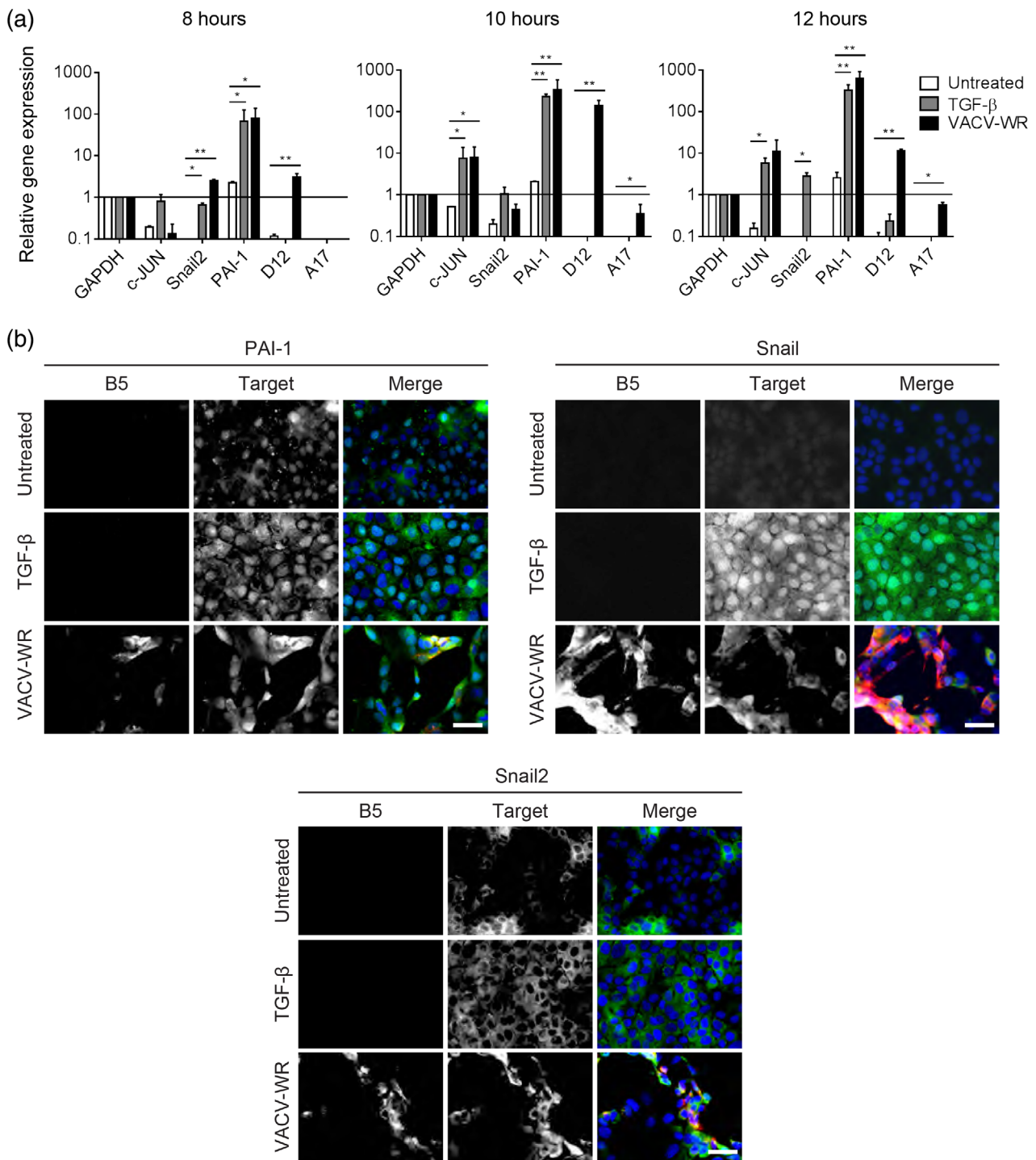


FIGURE 2 VACV infection induces expression of TGF- β response targets. (a) Expression of TGF- β -responsive genes by RT-qPCR in HaCaT cells at 8, 10 and 12 hpi with VACV-WR (MOI = 5) or treatment with TGF- β ($n = 3$, $*p < .05$, $**p < .01$ by unpaired t test). Error bars refer to SEM. (b) PAI-1 (top left), Snail (top right) and Snail2 (bottom) target expression in HaCaT cells at 8 hpi with VACV-WR (MOI = 5) or treatment with TGF- β . Scale bar = 50 μ m

reduced (Figure 4c). This was quantified as the area within the plaque devoid of cells (Figure 4a). This reduction in cell clearance at the centres of plaques is unlikely to result from a change in apoptotic activity in infected cells, as no changes in Caspase-3 activity were detected (Figure S2d). Live-cell tracking during VACV plaque formation

revealed a reduced rate of cell migration (Figure 4d) and cell displacement (Figure 4e) following Smad4 knockdown. VACV-infected HaCaT cells do not display abundant viral actin-based motility compared to other cell types. When virus release from infected cells was assayed, no significant difference was observed in Tet-treated and untreated

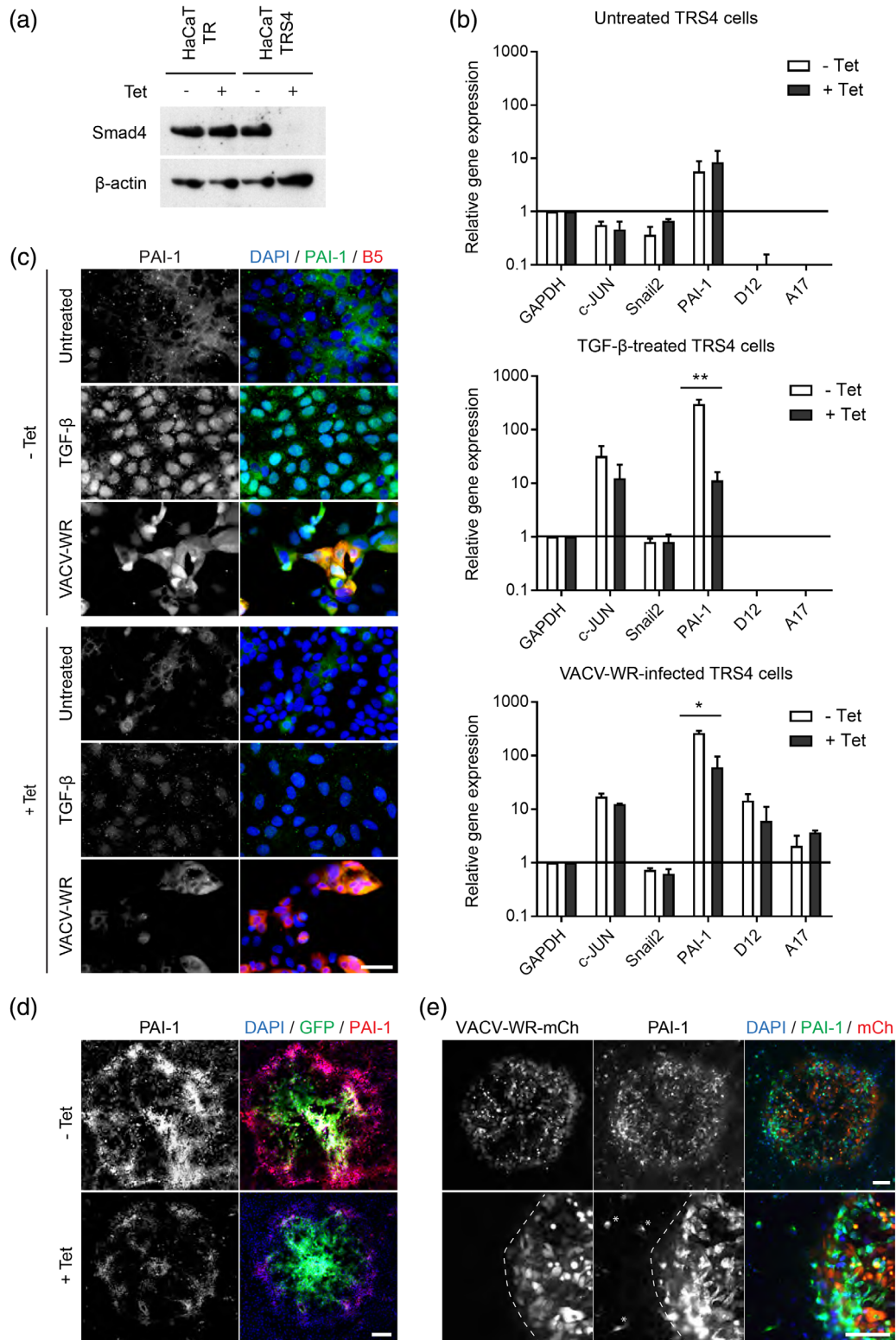


FIGURE 3 PAI-1 induction by VACV is Smad4-dependent. (a) Smad4 expression in HaCaT-TR and -TRS4 control cells following treatment with Tet for 48 hr. (b) Expression of TGF-β-responsive genes by RT-qPCR in HaCaT cells with reduced levels of Smad4 at 10 hpi with VACV-WR (MOI = 10) or treatment with TGF-β ($n = 4$, $*p < .05$, $**p < .01$ by unpaired t test). (c) Expression of PAI-1 (green) in HaCaT TRS4 cells at 10 hpi with VACV-WR (red) (MOI = 5) or treatment with TGF-β. (d) Micrograph of PAI-1 (red) expression within VACV-WR (LifeAct-GFP) plaques following Smad4 knockdown. Scale bar = 50 μm . (e) Representative image showing localisation of PAI-1 (green) expression in a VACV-WR (mCherry) plaque at $\times 40$ and $\times 200$ magnifications. PAI-1 expression is strongly induced within the plaque boundary (marked by dotted line). Induction of PAI-1 was also observed infrequently in uninfected cells (marked by asterisks). Scale bar = 100 μm

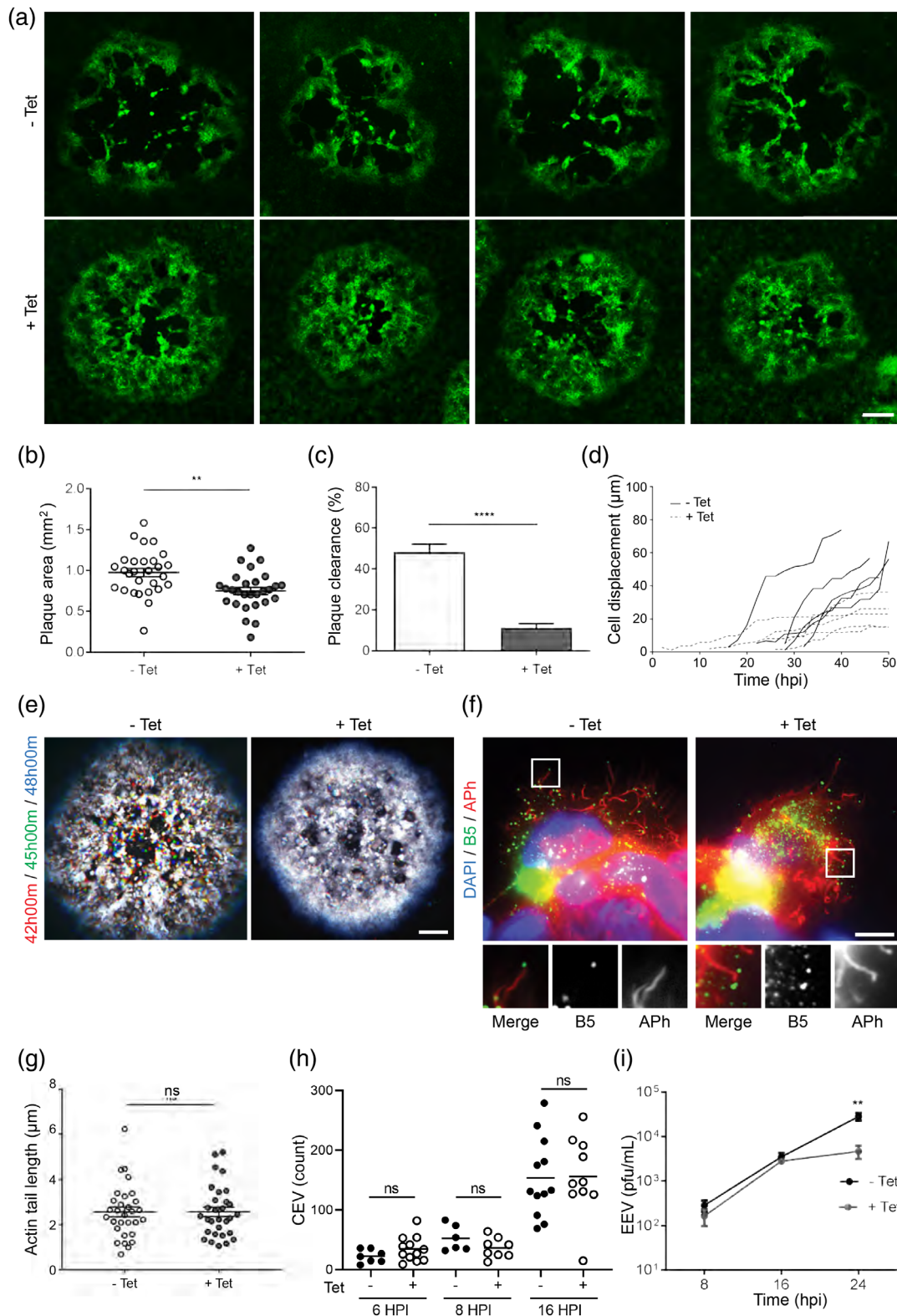


FIGURE 4 Smad4 is required for optimal cell-to-cell spread of VACV. (a) Representative micrographs of VACV-WR (LifeAct-GFP) plaques at 48 hpi formed in HaCaT TRS4 cells following Tet induction. Scale bar = 200 μm . (b,c) Diameter and area of cell clearance of plaques from (a). $n = 30$ plaques per condition ($*p < .05$, $**p < .01$, $****p < .001$ by unpaired t test). (d) Single-cell tracking of VACV-WR (mCherry)-infected HaCaT TRS4 cells. Tracks were generated using ImageJ software for 5 cells per condition ($n = 5$). (e) Three frame overlay of HaCaT TRS4 cells from 42 (red), 45 (green) and 48 (blue) hpi with VACV-WR (LifeAct-GFP). False colouring of each frame demonstrates reduced cell movement (fewer single-coloured cells) under conditions of Smad4 depletion. Scale bar = 100 μm . (f) Representative images of actin tail formation in HaCaT TRS4 cells following depletion of Smad4 (Scale bar = 5 μm). (g) Actin tail length at 16 hpi with VACV-WR (MOI = 5) in HaCaT TRS4 cells. Thirty tails were analysed (unpaired t test). (h) CEV counts at 6, 8 and 16 hpi with VACV-WR (MOI = 5) in HaCaT TRS4 cells (Ordinary one-way ANOVA with Tukey's multiple comparisons). (i) Extracellular virus release from HaCaT TRS4 cells at 8, 16 and 24 hpi with VACV-WR (MOI = 0.1, $n = 3$)

cells at 16 hpi. However, no significant differences in the efficiency of virus-induced actin nucleation nor morphology of virus-tipped actin comets were observed between control and Smad4-depleted conditions (Figure 4f,g). At 6, 8 and 16 hpi, there was also no observable difference in the number of CEV present on Tet-treated and

untreated cells (Figure 4h). At 24 hpi, Smad4 knockdown resulted in decreased virus release (Figure 4i), which suggests that replication dynamics are unaffected at the first round of replication but that subsequent cell-to-cell transmission may be disrupted. This is consistent with the expression of the viral transcripts D12 and A17 being

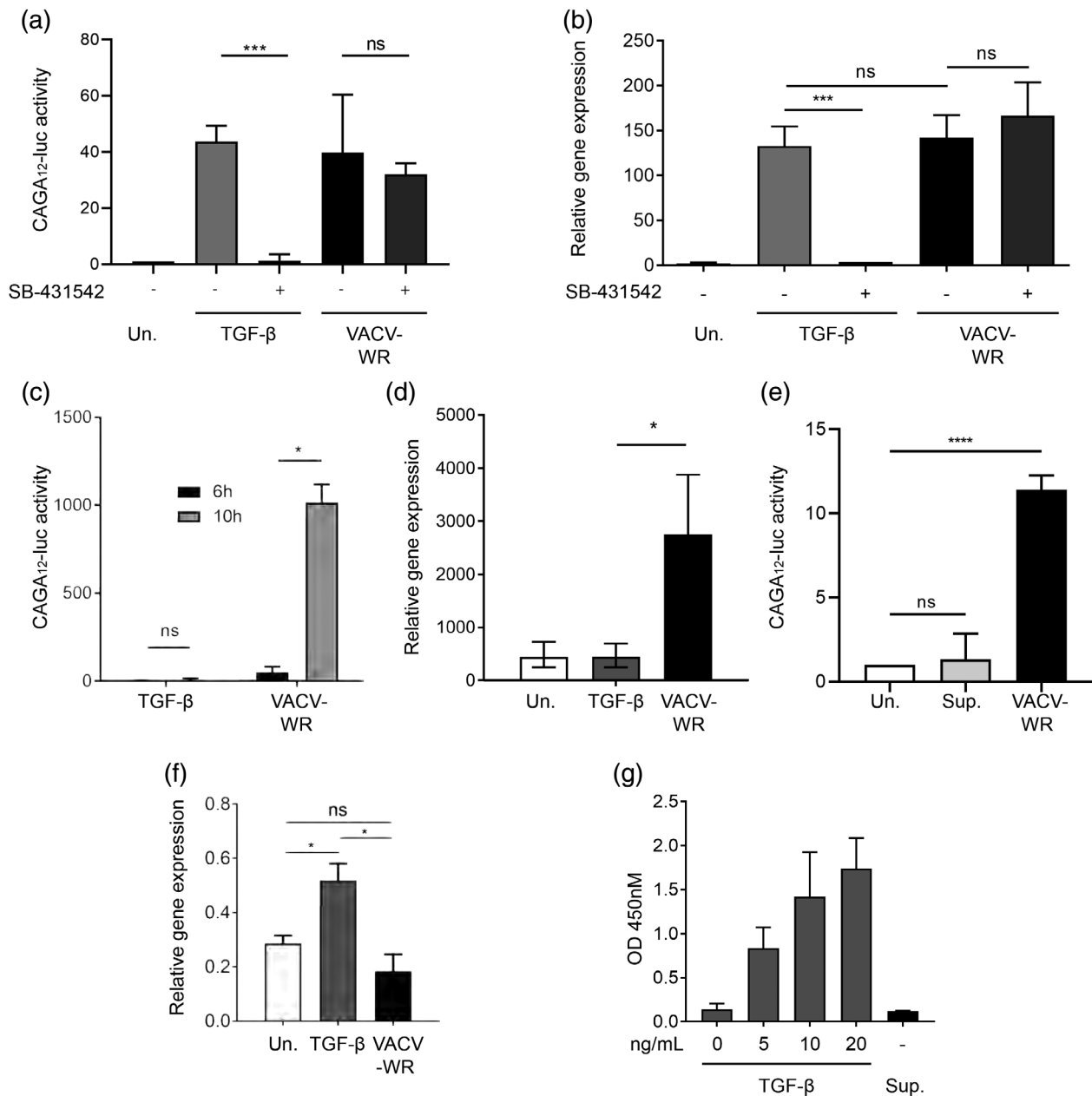


FIGURE 5 Activation of Smad signalling by VACV does not require the TGF- β receptor complex. (a) Activity of the CAGA₁₂-Luc reporter in HaCaT cells following treatment with SB-431542 at 8 hpi with VACV-WR (MOI = 10) or treatment with TGF- β (** p < .001 by One-way ANOVA with Tukey's multiple comparisons test). (b) Expression of PAI-1 mRNA in HaCaT cells by RT-qPCR following treatment with SB-431542, 8 hpi with VACV-WR (MOI = 5) or treatment with TGF- β (** p < .001 by unpaired t test). (c) Activity of the CAGA₁₂-Luc reporter in LNCaP cells following infection with VACV-WR (MOI = 5) or treatment with TGF- β . (d) RT-qPCR of PAI-1 mRNA in LNCaP cells 8 hpi with VACV-WR (MOI = 5) or treatment with TGF- β (* p < .05 by unpaired t test). (e) Activity of the CAGA₁₂-Luc reporter following treatment of HaCaT cells with VACV-WR supernatant (**** p < .0001 by One-way ANOVA with Tukey's multiple comparisons test). (f) Expression of TGF- β mRNA in HaCaT by RT-qPCR following infection with VACV (MOI = 5) or treatment with TGF- β (* p < .05 by unpaired t test). (g) Detection of secretion of TGF- β into the supernatant following infection with VACV-WR (MOI = 5) or treatment with TGF- β , as detected by ELISA (n = 3)

unaffected by Smad4 knockdown at 10 hpi (Figures 3b and S2a). Taken together with the replication dynamics, the lack of change in actin comet nucleation efficiency, our results are consistent with a defect in cell migration as contributing to the attenuated cell-to-cell spread.

To confirm that Smad signalling activation was not an artefact of infection of HaCaT cells in particular, we assayed the reporter activity in HeLa cells. All three TGF- β -responsive reporter elements (SBR, ARE, and CAGA₁₂) were upregulated following infection with VACV WR (Figure S3a–c). In order to test the requirement for Smad4 in virus spread in another cell line, we generated HeLa cells with loss-of-function lesions in Smad4. Cells were transfected with plasmids expressing Cas9 and a guide RNA (gRNA) designed to induce early frameshift mutations at the 5' end of Smad4 via non-homologous end-joining. Cells were sorted by GFP expression (co-expressed with Cas9) and the resulting mixed cell populations were tested for Smad4 expression and compared to cells that were treated with control gRNAs. Although this mixed cell population is predicted to comprise wild type, heterozygous and homozygous genotypes, the observed reduction in Smad4 levels revealed that Cas9 cleavage at the Smad4 locus was highly efficient (Figure S3f). VACV plaques formed in Smad4-edited HeLa cells displayed many of the same features as Smad4-depleted HaCaT cells, with a moderate, but significant reduction in plaque size and an observable reduction in clearing (Figure S3g,h).

2.4 | VACV induction of Smad-dependent signalling is independent of TGF- β receptors

We next examined the involvement of TGF- β in VACV-induced R-Smad/Smad4 signalling by testing the requirement for TGF- β receptors, TGFBR1 and TGFBR2. The small molecule SB-431542 potently inhibits the kinase activity of TGF- β superfamily type I activin receptor-like kinase receptors (ALK), including ALK4, ALK5 and ALK7, which are the primary TGFBR1 receptors for TGF- β and activin (Inman et al., 2002). Inhibition of TGFBR1 disables Smad2 and Smad3 phosphorylation, which is required for the assembly of active transcription complexes and transcriptional activity (Chacko et al., 2004; Souchelnytskyi et al., 1997). As expected, SB-431542 potently suppressed CAGA₁₂-Luc reporter activation and PAI-1 induction by TGF- β (Figure 5a,b). These same results were seen for c-JUN and Snail2 transcripts (data not shown). Surprisingly, we observed activity of the CAGA₁₂-Luc reporter and induction of PAI-1 expression in VACV-infected cells regardless of the presence of SB-431542. In HeLa cells, activation of the CAGA₁₂ reporter similarly occurred even in the context of treatment with SB-431542 (Figure S3d,e). These data suggest that VACV induces R-Smad/Smad4 activity by an atypical, TGF- β -independent, TGFBR1/TGFBR2-independent mechanism. To further support this hypothesis, we obtained the prostate cancer-derived LNCaP cell line that is insensitive to TGF- β as it lacks expression of TGFBR1 (Kim, Ahn, et al., 1996; Wilding, Zugmeier, Knabbe, Flanders, & Gelmann, 1989). In addition, TGFBR2 is only expressed

within these cells in response to specific androgen stimuli (Kim, Zelner, et al., 1996). While LNCaP cells were demonstrated to be insensitive to TGF- β , infection with VACV induced activation of the CAGA₁₂-Luc reporter and expression of c-JUN, Snail2 and PAI-1 (Figure 5c,d) and data not shown). Furthermore, virus-free supernatant from infected cells did not activate the CAGA₁₂-Luc reporter and no significant increase in TGF- β transcript or secreted TGF- β levels were observed following infection (Figure 5e–g). Collectively, these lines of evidence do not support a role for TGF- β or TGF- β receptors in promoting R-Smad/Smad4-mediated transcription upon VACV infection and propose a novel molecular mechanism for driving a TGF- β -like response.

2.5 | TGF- β enhances cell-to-cell spread of ECTV infection

The ability to induce a TGF- β -like response was found to be conserved among related VACV strains (Figure 1e). To determine whether this activity was conserved between different orthopoxviruses, we tested cells infected with ECTV-Moscow strain (ECTV-Mos). ECTV-infected cells did not lead to increased CAGA₁₂-Luc activity, nor were c-JUN and PAI-1 transcripts induced, unless exogenous TGF- β was additionally supplied (Figure 6a,b). Immunoblot analysis also revealed that Smad2 phosphorylation (S465/S467) was not elevated in ECTV-infected cell lysates (Figure 6c). Furthermore, Snail, Snail2 and PAI-1 expression was not increased in response to ECTV as compared to VACV infection, when cells were analysed by immunofluorescence (Figure 6d). Thus, none of the hallmarks of TGF- β signalling that we observed with TGF- β treatment or VACV infection were associated with ECTV infection. Accordingly, depletion of Smad4 in TRS4 cells did not attenuate ECTV plaque size indicating that Smad4 and Smad4-containing transcription complexes are not required for ECTV spread (Figure 6e,f). Attenuation of plaque size by Smad4-depletion was also not observed with HSV-1, an unrelated dsDNA virus. HSV-1 plaques formed under conditions of Smad4 depletion at 3 days post-infection (dpi) were not significantly different in diameter (–Tet = $0.62 \pm 0.07 \text{ mm}^2$ and +Tet = $0.75 \pm 0.08 \text{ mm}^2$, and data not shown). Thus, depletion of Smad4 does not attenuate the plaque size of dsDNA viruses in general but specifically perturbs VACV spread.

ECTV forms plaques that are reduced in size compared with those formed by VACV, which is partly due to a slower rate of replication (Lynn et al., 2012). However, ECTV plaques also display significantly different morphology to VACV plaques with cells congregating at the centre of plaques (Figure 7a). We postulated that the absence of TGF- β -like signalling may be partly responsible for the difference in plaque size and morphology between the two viruses. To test this hypothesis, we generated ECTV plaques in HaCaT cells in the presence of exogenous TGF- β . Treatment with TGF- β had a drastic effect on ECTV plaques, evoking a more VACV-like morphology with reduced cell clumping and resulting in a significant increase in plaque size (Figures 7a–c).

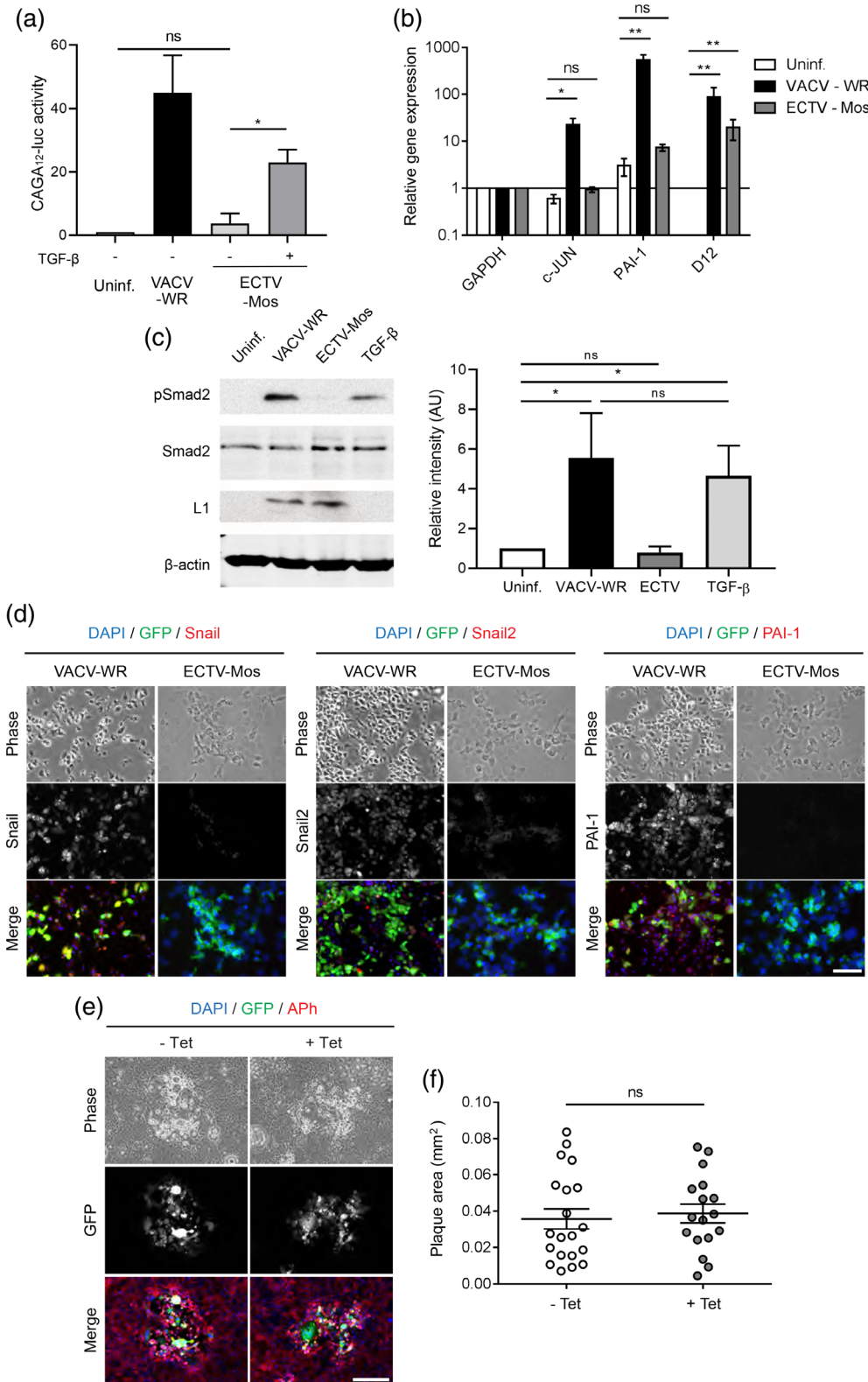
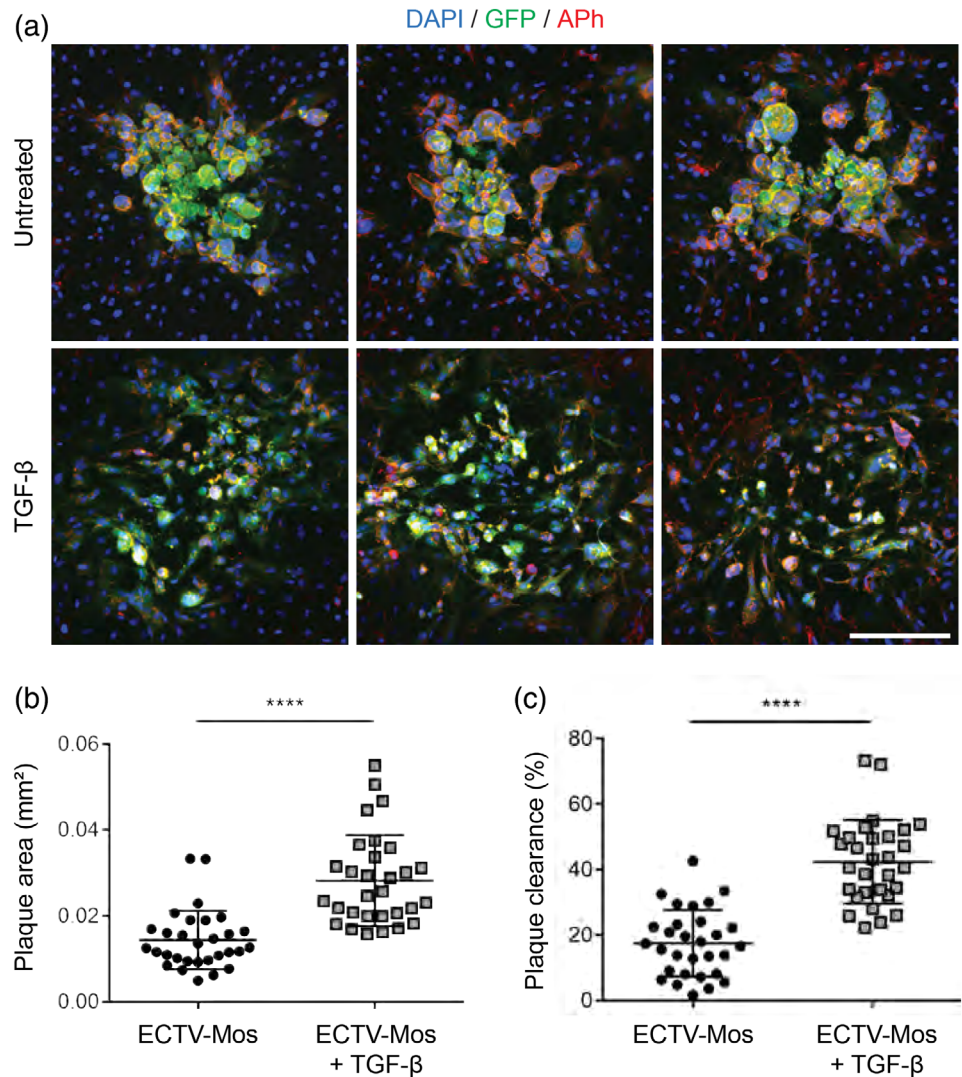


FIGURE 6 ECTV does not elicit TGF-β-like signalling during infection. (a) Activation of the CAGA₁₂-Luc reporter at 16 hpi with ECTV-Mos (MOI = 5) or 8 hpi with VACV-WR (MOI = 5). (b) RT-qPCR analysis of TGF-β target mRNAs at 16 hpi with ECTV-Mos (MOI = 10) (**p* < .05, ***p* < .01 by unpaired *t* test). (c) Phosphorylation of Smad2 (S465/S467) following infection with VACV-WR (8 hpi) or ECTV-Mos (16 hpi), or treatment with TGF-β. Images presented are representative of three independent experiments (**p* < .05 by One-way ANOVA with Tukey's multiple comparisons test). (d) Induction of TGF-β targets (red) following infection with ECTV-Mos (LifeAct-GFP) or VACV-WR (LifeAct-GFP). Scale bar = 50 μm. (e,f) Plaques formed by ECTV-Mos (LifeAct-GFP) in HaCaT TRS4 cells (5 dpi, *n* = 20). Actin is visualised in red (APh). Scale bar = 100 μm

FIGURE 7 Exogenous TGF- β enhances the spread of ECTV.

(a) Representative images of plaques formed by ECTV-Mos (Lifeact-GFP) with or without TGF- β treatment. Actin is visualised in red (Aph). Scale bar = 200 μ m. (b,c) Plaque area (b) and plaque clearance (c) following infection with ECTV-Mos (LifeAct-GFP) and treatment with TGF- β ($n = 30$ plaques per condition, **** $p < .001$ by unpaired *t* test)



3 | DISCUSSION

Virus spread in a complex three-dimensional tissue within a multicellular organism is determined by the speed of replication, the dynamics of virus release, and cell lysis. In addition, certain viruses have developed specialised mechanisms to enhance spread such as actin-based motility (VACV), the formation of the virological synapse (human immunodeficiency virus) and syncytia formation (respiratory syncytial virus) (Sattentau, 2008). The plaque assay is a powerful tool to elucidate the mechanisms that contribute to virus spread and, in the case of VACV, has revealed that the speed of plaque progression greatly outpaces replication dynamics (Doceul et al., 2010). In BSC-1 cells, the plaque front crosses a cell diameter every 1.2 hr, which is faster than a replication cycle of 5–6 hr would predict when diffusion of an extracellular virus is blocked with an overlay (Beerli et al., 2019; Doceul et al., 2010). Beerli et al. noted that infected cells traverse an average of 10 uninfected cells over the course of 24 hr (Beerli et al., 2019). In this study with plaque assays performed in HaCaT cells, we also observed speeds of cell-to-cell spread in HaCaT cells that are inconsistent with replication dynamics alone. Repulsion of

superinfecting virions—whereby extracellular virus leap-frogs early-stage infected cells—can contribute to virus spread to surpass replication kinetics (Doceul et al., 2010). Our data also support a role for Smad4-dependent virus-induced cell motility as a mechanism promoting virus spread.

We have shown that signalling mediated by Smad4 does not disrupt replication kinetics (Figure 4i) or actin-based motility (Figure 4f, g) but significantly reduces plaque spread by inhibiting cell migration (Figure 4a,d,e). Cells infected with VACV display a motile phenotype (Sanderson, Way, & Smith, 1998), which is accompanied by an inhibition of RhoA signalling and altered substrate adhesion (Cordeiro et al., 2009; Valderrama, Cordeiro, Schleich, Frischknecht, & Way, 2006). Expression of the viral protein F11 (encoded by F11L) is at least partially responsible for mediating these effects through direct binding with RhoA GTPase and the Rho GAP (GTPase activating protein) Myosin-9A (Handa, Durkin, Dodding, & Way, 2013; Valderrama et al., 2006). Stimulation of EGFR by VGF shed by infected cells acts in concert with F11 to promote the migration of infected cells and enhance virus spread both in vitro and in vivo (Beerli et al., 2019; Cordeiro et al., 2009). With our data, we propose that the TGF-

β /Smad pathway, in addition to VGF/EGFR, dynamically and spatially fine-tunes cytoskeletal function and contributes to VACV-induced cell migration. These pathways must be orchestrated in concert with cellular changes that promote invasiveness and regulate substrate and cell-to-cell adhesion. An important finding was the observation of Smad4-dependent induction of PAI-1. PAI-1 is a member of the serpin superfamily that inhibits the conversion of plasminogen to plasmin by uPA and tPA proteases. PAI-1 was strongly induced in VACV-infected cells, significantly above background levels where PAI-1 expression infrequently induced in isolated cells. The cellular effects of PAI-1 are highly context-dependent and can promote both increased and decreased cell adhesion and migration (Kwaan, Wang, Svoboda, & Declerck, 2000). A loss of PAI-1 activity has been shown to reduce migration, particularly in human keratinocytes (Li et al., 2000; Providence & Higgins, 2004). Snail transcription factors are also important regulators of EMT and cytoskeletal rearrangements and are induced by TGF- β , Wnt and BMP ligands (Bi, Jin, Xu, & Yang, 2012; Haraguchi, 2009; Yook, Li, Ota, Fearon, & Weiss, 2005). Snail proteins regulate cell migration via integrin expression and attachment to the extracellular matrix (Haraguchi, 2009). Another target of interest, c-Jun is a component of the AP-1 transcription complex whose pleiotropic functions include roles in proliferation and cell migration (Shaulian, 2010). The activity of c-Jun is regulated during VACV infection by a mitogen-activated kinase (MAPK) and c-Jun N-terminal kinase (JNK) signalling (Leite et al., 2017) and plays a role in virus replication and cytoskeletal organisation (Leite et al., 2017; Pereira et al., 2012). We propose that during VACV infection, TGF- β and VGF signalling induces a migratory and EMT-like phenotype while F11 directly regulates the cytoskeleton, which, when combined, enhances cell motility.

The induction of TGF- β signalling by the direct expression of TGF- β has been previously observed during infection with ebolavirus, reovirus, HCV and HBV (Guo, Tan, Zhu, & Liu, 2009; Kim, Lee, & Lee, 2016; Kindrachuk et al., 2014; Stanifer et al., 2016). Others, such as fowlpox and deerpox virus, produce a homologue of TGF- β to act on this pathway (Afonso et al., 2000; Afonso et al., 2005). However, we could find no evidence to support a role for TGF- β itself, a homologue or TGF- β receptors in mediating the TGF- β -response we observed in VACV-infected cells. This was a surprising result as serine phosphorylation of R-Smads at the SSXS motif is thought to be essential for the recruitment of Smad4 and the formation of an active transcription complex (Kamoto et al., 2013; Souchelnytskyi et al., 1997; Wrighton et al., 2009). Although R-Smads are targets of a number of kinases, such as MAPK, these are thought to primarily modulate activity post-TGFBR1 phosphorylation (Hayashida, Decaestecker, & Schnaper, 2003; Rostam et al., 2016; Souchelnytskyi et al., 1997). None of these kinases possess activity for the SSXS motif. There are some reports of induction of Smad-mediated EMT by EGF/MAPK but in these cases, the activity of TGF- β and its cognate receptors were not assayed (Kim, Kong, Chang, Kim, & Kim, 2016). Given that VACV produces an EGF homologue, VGF, it is possible that EGF pathway cross-talk contributes to Smad signalling during VACV infection; however, EGF signalling itself is not capable of initiating TGF- β responses

via SSXS phosphorylation (Beerli et al., 2019; Twardzik, Brown, Ranchalis, Todaro, & Moss, 1985). Recent work has shown that VGF is indeed involved in directing infected cell motility, via ERK/MAPK intermediaries (Beerli et al., 2019). It may be that VGF-initiated ERK/MAPK signalling is involved in modulating the TGF- β -like response observed in VACV-infected cells to promote cell migration. The mechanism for the apparent independence of pathway activity to TGF- β or the TGF- β receptors is still unclear. The only report, to our knowledge, of a kinase other than TGFBR1 with activity towards the R-Smad SSXS motif is Mps1, which phosphorylates Smad2 and Smad3 in nocodazole-treated cells (Zhu, Wang, Clarke, & Liu, 2007). Although an Mps1 inhibitor did not affect VACV-stimulation of R-Smad signalling (data not shown), this raises the possibility of hitherto unidentified kinases that can elicit a TGF- β transcriptional response. We believe that VACV might prove to be a key reagent to uncover such a mechanism.

It is well known that TGF- β plays a highly pleiotropic and nuanced role within the contexts of development and oncogenesis. Similarly, the manipulation of TGF- β signalling by viral agents can be just as delicately refined. For instance, damage to the epithelial barrier of the respiratory tract triggers EMT and TGF- β expression and suppresses the type I and type III interferon response (Yang, Tian, Sun, Garofalo, & Brasier, 2017). This leads to increased sensitivity to respiratory syncytial virus and rhinovirus infection. HCV is known to upregulate TGF- β , the direct result of which is the suppression of IL-17-secreting T cells. The downstream effect of this is an increased contribution to the acceleration of fibrosis and an increased risk of hepatocellular carcinoma and metastasis in infected patients (Meindl-Beinker, Matsuzaki, & Dooley, 2012; Rowan et al., 2008). Infection of intestinal epithelial cells with mammalian reovirus intermediate subviral particles—proteolytically cleaved virions—leads to the secretion of TGF- β that exerts a pro-survival signal. This response is highly cell type specific and exclusive to polarised epithelial cells. The pro-survival signal counteracts the induction of apoptosis by reovirus virions and extends the interval of productive virus infection (Stanifer et al., 2016). Induction of TGF- β by ebolavirus leads to expression of EMT markers associated with tissue plasticity. In this context, inhibition of the TGFBR1 with SB-431542 leads to decreased virus replication *in vitro* and rescues lethally infected BALB/c mice (Kindrachuk et al., 2014). The authors propose that the loss of epithelial cell integrity and motility of infected cells contributes to the spread of ebolavirus infection. We believe this model best describes the role of induction of TGF- β /Smad signalling by VACV, albeit via a TGFBR1-independent mechanism.

TGF- β can display either tumour-promoting or tumour-suppressing activity depending on the context. High levels of TGF- β are associated with many clinical tumours and, conversely, mutations in Smad4 are often described as oncogenic (Akhurst & Hata, 2012; Caja, Kahata, & Moustakas, 2012). Pro-oncogenic pathways, including expression of thymidine kinase and suppression of apoptosis, are pro-viral and many cancer cell lines are highly productive for the replication of DNA and RNA viruses. Viral tropism for cancer cells forms the basis for oncolytic therapy. VACV has demonstrated activity as an oncolytic virus and its natural affinity for cancer cells can be enhanced

by mutations in virally encoded genes involved in nucleotide synthesis (thymidine kinase), apoptosis (F1L, B22R), cell proliferation (VGF) and ribonucleotide reductase (F4L) (Ilkow, Swift, Bell, & Diallo, 2014; Potts et al., 2017). We have shown that exogenous TGF- β can enhance the spread of ECTV, an orthopoxvirus that does not activate TGF- β signalling. This observation suggests that activation of TGF- β signalling is able to be parsed from virus viability and that the ability to induce EMT and cell restructuring and migration is an additional pathway with the potential to refine tumour selectivity of oncolytic poxviruses. A number of cancers are associated with high levels of TGF- β including colon, prostate, breast, lung and hepatocellular carcinomas for which a TGF- β pathway-selective oncolytic virus might have utility (Calon et al., 2012; Teicher, 2001; Vo et al., 2013).

4 | EXPERIMENTAL PROCEDURE

4.1 | Cell lines

Human keratinocyte (HaCaT), African Green monkey kidney epithelium (BSC-1, ATCC CCL-26), human cervical cancer (HeLa, ATCC CCL-2) and human pancreatic carcinoma (PANC-1, ATCC CRL-1469) cells were maintained in Dulbecco's Modified Eagle's Medium (DMEM; Life Technologies). Human prostate cancer (LNCaP, ATCC CRL-1740) and human colorectal adenocarcinoma cells (HT-29, ATCC HTB-38) were grown in Roswell Park Memorial Institute medium (RPMI; Life Technologies) and McCoy's 5A modified media (Gibco), respectively. All media were supplemented with 10% foetal bovine serum (FBS), 292 $\mu\text{g}/\text{mL}$ L-glutamine, 100 units/mL penicillin and 100 units/mL streptomycin (DMEM-FPSG) and incubated at 37°C and 5% CO₂, except for BSC-1 cells, which were supplemented with 5% foetal bovine serum. RPMI medium was additionally supplemented with 1 mM sodium pyruvate.

The previously described human keratinocyte (HaCaT) cell lines, HaCaT TR and HaCaT TRS4 (Levy & Hill, 2005), were maintained in DMEM-FPSG, supplemented with blasticidin (100 $\mu\text{g}/\text{mL}$). The HaCaT TRS4 cell media was additionally supplemented with zeocin (400 $\mu\text{g}/\text{mL}$). For inducible Smad4 knockdown, tetracycline (2 $\mu\text{g}/\text{mL}$) was added to cells 48 hr prior to use. Efficient knockdown was validated via immunoblot.

4.2 | CRISPR-Cas9 editing of Smad4

gRNAs for Smad4 were selected using the CRISPR design tool (<http://crispr.mit.edu/>) (Ran et al., 2013) and, along with control gRNAs for non-related target EMX1, were cloned into the pSpCas9(BB)-2A-GFP vector (Addgene #48138). HeLa cells were transfected with the resulting plasmids and sorted for GFP expression by FACS (BD FACSAria IIu). Mixed cell populations were confirmed by RFLP analysis and immunoblotting. gRNA sequences used were 5'-CACCTACAGAGAACATTGGATGGG-3' (Smad4G3) and 5'-CACCTTCTTCTGCTCGGACTC-3' (EMX1).

4.3 | Viruses

The viruses used in this study are VACV-Western Reserve strain (ATCC VR-1354), VACV-Copenhagen strain (VACV-Cop), VACV-Lister strain (ATCC VR-862), VACV-Chorioallantois virus Ankara (VACV-CVA) and ECTV-Moscow strain (ATCC VR-1374). The following viruses were used for imaging: VACV-WR (LifeAct-GFP), VACV-WR (mCherry) and ECTV-Mos (LifeAct-GFP). VACV-WR (LifeAct-GFP) has been previously published (Marzook et al., 2017), VACV-WR (mCherry) and ECTV-Mos (LifeAct-GFP) were constructed using a recombination cassette carrying pE/L-mCherry or pE/L-LifeAct-GFP in addition to a functional copy of viral gene A36R or 137.5 (Chakrabarti, Sisler, & Moss, 1997). Cells were infected with VACV Δ A36R or ECTV Δ 137.5, transfected with recombination plasmids and successful recombinants were selected by the rescue of the Δ A36R or Δ 137.5 small plaque phenotype and screening for fluorescence.

Virus infections were conducted by applying virus suspended in serum-free DMEM medium (SFM) to cells washed with phosphate-buffered saline (PBS). After 1 hr incubation at 37°C with 5% CO₂, the cells were recovered by replacing the virus suspension with fresh growth medium. For TGF- β treatment, cells were treated as for virus infections except that 2 $\mu\text{g}/\text{mL}$ TGF- β (Peprotech) was added to both the SFM and recovery medium. Inhibition of TGF- β signalling during infection was achieved by including SB-431542 (10 μM) (Tocris) in the infection and recovery medium.

For experiments requiring the treatment of cells with viral supernatants, cells were infected with VACV-WR at a MOI of 10 for 24 hr and supernatant growth medium recovered. This supernatant was filtered using a 0.2 μm syringe filter (Millipore) and applied to a fresh monolayer of HaCaT cells. Removal of extracellular virions was confirmed by plaque assay.

4.4 | Elisa

For ELISA analysis of cell supernatants, HaCaT cells were grown to confluency in six-well dishes prior to 24 hr of serum starvation. At this point, TGF- β treatments or VACV-WR infections were applied in SFM as previously described. Supernatants were collected at specified time points and used alongside the Human TGF- β 1 ELISA Kit (Sigma-Aldrich) according to the manufacturer's instructions. A standard curve was generated using the supplied control standard. Samples were analysed using the Spark Multimode Microplate reader (Tecan) and SparkControl software (Tecan, v2.3).

4.5 | Imaging

BSC-1, HaCaT, PANC-1 and HT-29 cells were grown on glass coverslips and infected with virus strains as described. Coverslips were fixed at the appropriate time post infection with paraformaldehyde (PFA) in a cytoskeletal buffer (CB) [10 mM 2-(*N*-morpholino)

ethanesulfonic acid (MES) buffer, 0.15 M NaCl, 5 mM ethylene glycol tetraacetic acid (EGTA), 5 mM MgCl₂, 50 mM glucose, pH 6.1]. Antibodies were used to visualise cellular proteins including Snail (Santa Cruz Antibodies, H-130), Snail2 (Santa Cruz Antibodies, H-140), PAI-1 (Santa Cruz Antibodies, C-9), as well as, viral protein, B5 (19C2) (Cudmore, Cossart, Griffiths, & Way, 1995). Slides were visualised using an Olympus BX51 Microscope with Reflection Fluorescence System, Mercury Burner (U-RFL-T), F-view monochrome fluorescence camera and DAPI (347 nm/442 nm [#31013v2]), eCFP (436 nm/480 nm [#49001]), FITC (495 nm/515 nm [#31001]) and TxRed (584 nm/610 nm [#31004]) Chroma filters. Micrographs were captured using AnalySIS LS Starter (Olympus Soft Imaging Systems, v2.8) and processed using ImageJ (NIH, v1.47i).

Live cell imaging was conducted on the Nikon Ti-E eclipse microscope using the NIS Elements microscope imaging software (AR 4.51.00) and iXON Ultra 888 EMCCD camera (Andor). The light was supplied by a Lumencor Spectra X fluorescent light source and passed through Semrock standard filters: DAPI, eCFP, FITC and TxRed. For the duration of imaging, cells were maintained at 37°C, 5% CO₂ and 85% humidity. Following imaging, analyses were performed using ImageJ software and GraphPad Prism 7 (GraphPad Software Inc, v7.0).

4.6 | Luciferase assay

Cultured cells were transfected with a luciferase reporter and *Renilla* control plasmids for luciferase assays. Firefly luciferase reporter plasmids used in this study (ARE-luc, SBR-luc and CAGA₁₂-luc) have been previously described (Levy & Hill, 2005). All firefly luciferase reporter constructs were kindly provided by Caroline Hill (Cancer Research UK). For Figures 1(d,e) and 5(a,e) a HaCaT line with stable expression of CAGA₁₂-firefly and TK-*Renilla* luciferase was used. This cell line has been described in a previous study (Levy et al., 2007). Luciferase reporter assays were performed approximately 48 hr after transfection using the Dual-Luciferase Reporter Assay System (Promega), in accordance with the manufacturer's instructions. Luciferase activity was measured using a TD-20/20 luminometer (Turner Designs). Immunofluorescence assays were performed in parallel to confirm infection by detection of viral protein B5.

4.7 | Immunoblot

Cells were washed in chilled PBS and harvested on ice in sodium dodecyl sulfate (SDS)-reducing sample buffer (62.5 mM Tris-HCl, 0.25 M glycerol, 2% SDS, 0.01% [wt/vol] bromophenol blue, 12.5% [vol/vol] β-mercaptoethanol) and boiled three times at 95°C for 3 min. Proteins were separated by SDS-polyacrylamide gel electrophoresis (SDS-PAGE) (resolving gel of 10% acrylamide-Bis solution [37.5:1], 0.375 M Tris-HCl, pH 8.8, 0.1% [wt/vol] SDS, 0.1% ammonium persulfate (APS) and 0.1% *N,N,N',N'*-tetramethylethylenediamine [TEMED]; stacking gel of 4% to 30% acrylamide-Bis solution [37.5:1],

0.375 M Tris-HCl, pH 6.8, 0.1% [wt/vol] SDS, 0.1% APS and 0.1% TEMED). Separated proteins were transferred to a nitrocellulose membrane (Hybond-C Extra; Amersham Biosciences) by electroblotting. Membranes were probed with primary antibodies in PBST-Milk (5% [wt/vol] skim milk powder in PBS with 0.1% Tween 20), or TBST-BSA (5% [wt/vol] BSA in TBS with 0.1% Tween 20) for detection of phosphorylated proteins. Monoclonal primary antibodies specific to Smad2 (86F7), p-Smad2 (138D4), Smad3 (C67H9) and p-Smad3 (C25A9) were purchased from Cell Signalling Technology (Danvers, MA). Antibodies specific to β-actin (Sigma-Aldrich, AC-74) and viral proteins A36 (Rottger, Frischknecht, Reckmann, Smith, & Way, 1999) and L1 (BEI Resources, NR-631) were also used. Membranes were washed three times in TBST-BSA and then probed with appropriate secondary antibodies conjugated to horseradish peroxidase (Santa Cruz). Protein bands were visualised by enhanced chemiluminescence (ECL) reagent (GE Healthcare).

4.8 | Plaque assay

HaCaT cells were seeded in six-well plates and grown to confluence. Virus strains were diluted in SFM and a 10-fold serial dilution of virus stock was added to the wells. Cells were incubated at 37°C in 5% CO₂ for 1 hr and then washed before being overlaid with 1.5% carboxy-methyl cellulose (CMC) in minimal essential medium (MEM) (Life Technologies) supplemented with 292 μg/mL L-Glutamine, 100 units/mL penicillin, 100 units/mL streptomycin and 10% FBS. VACV plaques were allowed to form for 2–3 days before being examined, while ECTV plaques were allowed to form for 4–5 days. Additional ligands or chemical reagents were added to both the infecting medium and overlay as described. For visualisation of plaque morphology by fluorescence microscopy, the CMC overlay was removed by aspiration and coverslips were washed three times in PBS and processed as described above for immunofluorescence assays. Plaque size and clearance measurements were performed using ImageJ software. Briefly, plaques edges were outlined via detection of cytopathic effect or presence of fluorescence, depending on the virus being used. This outline was used to measure the plaque area using ImageJ software (also referred to as plaque size within this paper). For measuring plaque clearance, the threshold function on Image J software was used to determine the area within these plaques occupied by cells. When this number was subtracted from the total plaque area, this provided a measurement for the clear space within plaques. This was represented as a percentage of the total plaque area and was referred to as plaque clearance.

4.9 | EEV release assay

Extracellular virus release was measured via EEV release assay. Appropriate cells were grown to confluency in DMEM-FPSG media and infected at a MOI of 0.1 for 1 hr. At this point, media was removed, cells were washed in PBS and fresh media was added. At the specified

time points, cell supernatant was removed and viral titre was determined via plaque assay.

4.10 | CEV analysis

HaCaT TRS4 cells were seeded onto coverslips and treated and infected (with VACV-WR at MOI = 5) as previously described. At times indicated, cells were fixed with paraformaldehyde in CB as previously described. Coverslips were probed with rat anti-B5 (19C2, 1:300) before being washed and stained with anti-rat-Alexa488 secondary antibody (1:200). Cells were then permeabilised with 0.1% Triton in CB prior to staining with Phalloidin-Alexa568 (1:100) and DAPI (1 µg/mL). Coverslips were mounted with MOWIOL and imaged using an Olympus BX51 microscope as described previously. Micrographs were captured using AnalySIS LS Starter (Olympus Soft Imaging Systems, v2.8) and CEV counts were obtained using ImageJ (NIH, v1.47i).

4.11 | RNA extraction and quantitative RT-PCR

Appropriate cell types were grown to confluency in six-well plates and treated or infected as previously described. Total RNA was isolated using TRIzol Reagent (Life Technologies) before being treated with RQ1 RNase-Free DNase (Promega). cDNA was synthesised with a Superscript VILO™ cDNA synthesis kit (Invitrogen). Quantitative real-time PCR (RT-qPCR) assays were performed on a 7,500 using Fast Real-time PCR System (Life Technologies) using FastSYBR Green Master Mix (Life Technologies). The RT-qPCR primers used were: GAPDH FW 5'-GGAGTCAACGGATTTGGTCGTA-3', GAPDH REV 5'-GGCAACAATATCCACTTTACCAGAGT-3'; c-JUN FW 5'-TCCA CGGCCAACATGCT-3', c-JUN REV 5'-CCACTGTAACTGGTTCATGAC-3'; Snail2 FW 5'-ATACCACAACCAGAGATCCTCA-3', Snail2 REV 5'-GACTCACTCGCCCCAAAGATG-3'; PAI-1 FW 5'-CCGGAACAGCCTGAAGAAGTG-3', PAI-1 REV 5'-GTGTTTCAGCAGGTGGCGC-3'; TGFβ1 FW 5'-ACCTGAACCCGTGTTGCTCT-3', TGFβ1 REV 5'-CTAAGGCGAAAGCCCTCAAT-3'; D12 FW 5'-ACCTCAGCGCAGCAATAAACTGTTCA-3', D12 REV 5'-AGTCATACTAGAATAAAGCAGCGAGT-3'; A17 FW 5'-ATGAGTTATTTAAGATATTACAATATGCTT-3', A17 REV 5'-TCGTCAGTATTTAACTGTTAAATGTTGGT-3'. Each biological replicate was run in duplicate at two dilutions and overall expression levels were normalised to GAPDH for analysis. All analyses were performed using GraphPad Prism 7 software and Student's unpaired t test.

ACKNOWLEDGEMENTS

LNcaP cells were obtained from collaborator Stephen Assinder (University of Sydney, Australia). PANC-1 and HT-29 cells were from Des Richardson (University of Sydney, Australia). All firefly luciferase reporter constructs were kindly provided by Caroline Hill (Cancer Research UK). A.G., C.R.A., C.M., W.S.C., and T.P.N. performed and designed the experiments. A.G., C.R.A., and T.P.N. wrote and prepared the manuscript. G.K., L.L. and T.P.N. designed the study. This work

was in part supported by National Health and Medical Research Council Project Grant 632785.

CONFLICT OF INTEREST

The authors declare no competing interests.

ORCID

Timothy P. Newsome  <https://orcid.org/0000-0002-2193-596X>

REFERENCES

- Afonso, C. L., Delhon, G., Tulman, E. R., Lu, Z., Zsak, A., Becerra, V. M., ... Rock, D. L. (2005). Genome of deerpox virus. *Journal of Virology*, 79(2), 966–977. <https://doi.org/10.1128/JVI.79.2.966-977.2005>
- Afonso, C. L., Tulman, E. R., Lu, Z., Zsak, L., Kutish, G. F., & Rock, D. L. (2000). The genome of fowlpox virus. *Journal of Virology*, 74(8), 3815–3831.
- Akhurst, R. J., & Hata, A. (2012). Targeting the TGFβ signalling pathway in disease. *Nature Reviews. Drug Discovery*, 11(10), 790–811. <https://doi.org/10.1038/nrd3810>
- Beerli, C., Yakimovich, A., Kilcher, S., Reynoso, G. V., Flaschner, G., Muller, D. J., ... Mercer, J. (2019). Vaccinia virus hijacks EGFR signalling to enhance virus spread through rapid and directed infected cell motility. *Nature Microbiology*, 4(2), 216–225. <https://doi.org/10.1038/s41564-018-0288-2>
- Bi, W. R., Jin, C. X., Xu, G. T., & Yang, C. Q. (2012). Bone morphogenetic protein-7 regulates snail signaling in carbon tetrachloride-induced fibrosis in the rat liver. *Experimental and Therapeutic Medicine*, 4(6), 1022–1026. <https://doi.org/10.3892/etm.2012.720>
- Bidgood, S. R., & Mercer, J. (2015). Cloak and dagger: Alternative immune evasion and modulation strategies of poxviruses. *Viruses*, 7(8), 4800–4825. <https://doi.org/10.3390/v7082844>
- Bourquain, D., Dabrowski, P. W., & Nitsche, A. (2013). Comparison of host cell gene expression in cowpox, monkeypox or vaccinia virus-infected cells reveals virus-specific regulation of immune response genes. *Virology Journal*, 10, 61. <https://doi.org/10.1186/1743-422X-10-61>
- Brown, J. P., Twardzik, D. R., Marquardt, H., & Todaro, G. J. (1985). Vaccinia virus encodes a polypeptide homologous to epidermal growth factor and transforming growth factor. *Nature*, 313(6002), 491–492.
- Caja, L., Kahata, K., & Moustakas, A. (2012). Context-dependent action of transforming growth factor beta family members on normal and cancer stem cells. *Current Pharmaceutical Design*, 18(27), 4072–4086.
- Calon, A., Espinet, E., Palomo-Ponce, S., Tauriello, D. V., Iglesias, M., Cespedes, M. V., ... Batlle, E. (2012). Dependency of colorectal cancer on a TGF-beta-driven program in stromal cells for metastasis initiation. *Cancer Cell*, 22(5), 571–584. <https://doi.org/10.1016/j.ccr.2012.08.013>
- Cayrol, C., & Flemington, E. K. (1995). Identification of cellular target genes of the Epstein-Barr virus transactivator Zta: Activation of transforming growth factor beta igh3 (TGF-beta igh3) and TGF-beta 1. *Journal of Virology*, 69(7), 4206–4212.
- Chacko, B. M., Qin, B. Y., Tiwari, A., Shi, G., Lam, S., Hayward, L. J., ... Lin, K. (2004). Structural basis of heteromeric smad protein assembly in TGF-beta signaling. *Molecular Cell*, 15(5), 813–823. <https://doi.org/10.1016/j.molcel.2004.07.016>
- Chaikuad, A., & Bullock, A. N. (2016). Structural basis of intracellular TGF-beta signaling: Receptors and smads. *Cold Spring Harbor Perspectives in Biology*, 8(11), 1–17. <https://doi.org/10.1101/cshperspect.a022111>
- Chakrabarti, S., Sisler, J. R., & Moss, B. (1997). Compact, synthetic, vaccinia virus early/late promoter for protein expression. *BioTechniques*, 23(6), 1094–1097.
- Cho, H. J., Baek, K. E., Saika, S., Jeong, M. J., & Yoo, J. (2007). Snail is required for transforming growth factor-beta-induced epithelial-mesenchymal transition by activating PI3 kinase/Akt signal pathway.

- Biochemical and Biophysical Research Communications*, 353(2), 337–343. <https://doi.org/10.1016/j.bbrc.2006.12.035>
- Condit, R. C., Moussatche, N., & Traktman, P. (2006). In a nutshell: Structure and assembly of the vaccinia virion. *Advances in Virus Research*, 66, 31–124. [https://doi.org/10.1016/S0065-3527\(06\)66002-8](https://doi.org/10.1016/S0065-3527(06)66002-8)
- Cordeiro, J. V., Guerra, S., Arakawa, Y., Dodding, M. P., Esteban, M., & Way, M. (2009). F11-mediated inhibition of RhoA signalling enhances the spread of vaccinia virus in vitro and in vivo in an intranasal mouse model of infection. *PLoS One*, 4(12), e8506. <https://doi.org/10.1371/journal.pone.0008506>
- Cudmore, S., Cossart, P., Griffiths, G., & Way, M. (1995). Actin-based motility of vaccinia virus. *Nature*, 378(6557), 636–638. <https://doi.org/10.1038/378636a0>
- Dennler, S., Itoh, S., Vivien, D., ten Dijke, P., Huet, S., & Gauthier, J. M. (1998). Direct binding of Smad3 and Smad4 to critical TGF beta-inducible elements in the promoter of human plasminogen activator inhibitor-type 1 gene. *The EMBO Journal*, 17(11), 3091–3100. <https://doi.org/10.1093/emboj/17.11.3091>
- Doceul, V., Hollinshead, M., van der Linden, L., & Smith, G. L. (2010). Repulsion of superinfecting virions: A mechanism for rapid virus spread. *Science*, 327(5967), 873–876. <https://doi.org/10.1126/science.1183173>
- Doms, R. W., Blumenthal, R., & Moss, B. (1990). Fusion of intra- and extracellular forms of vaccinia virus with the cell membrane. *Journal of Virology*, 64(10), 4884–4892.
- Fenner, F. (1993). Smallpox: Emergence, global spread, and eradication. *History and Philosophy of Life Sciences*, 15(3), 397–420.
- Guo, G. H., Tan, D. M., Zhu, P. A., & Liu, F. (2009). Hepatitis B virus X protein promotes proliferation and upregulates TGF-beta1 and CTGF in human hepatic stellate cell line, LX-2. *Hepatobiliary & Pancreatic Diseases International*, 8(1), 59–64.
- Handa, Y., Durkin, C. H., Dodding, M. P., & Way, M. (2013). Vaccinia virus F11 promotes viral spread by acting as a PDZ-containing scaffolding protein to bind myosin-9A and inhibit RhoA signaling. *Cell Host & Microbe*, 14(1), 51–62. <https://doi.org/10.1016/j.chom.2013.06.006>
- Haraguchi, M. (2009). The role of the transcriptional regulator snail in cell detachment, reattachment and migration. *Cell Adhesion & Migration*, 3(3), 259–263.
- Hatakeyama, M. (2008). Linking epithelial polarity and carcinogenesis by multitasking helicobacter pylori virulence factor CagA. *Oncogene*, 27(55), 7047–7054. <https://doi.org/10.1038/onc.2008.353>
- Hayashida, T., Decaestecker, M., & Schnaper, H. W. (2003). Cross-talk between ERK MAP kinase and Smad signaling pathways enhances TGF-beta-dependent responses in human mesangial cells. *The FASEB Journal*, 17(11), 1576–1578. <https://doi.org/10.1096/fj.03-0037fje>
- Ilkow, C. S., Swift, S. L., Bell, J. C., & Diallo, J. S. (2014). From scourge to cure: Tumour-selective viral pathogenesis as a new strategy against cancer. *PLoS Pathogens*, 10(1), e1003836. <https://doi.org/10.1371/journal.ppat.1003836>
- Inman, G. J., Nicolas, F. J., Callahan, J. F., Harling, J. D., Gaster, L. M., Reith, A. D., ... Hill, C. S. (2002). SB-431542 is a potent and specific inhibitor of transforming growth factor-beta superfamily type I activin receptor-like kinase (ALK) receptors ALK4, ALK5, and ALK7. *Molecular Pharmacology*, 62(1), 65–74.
- Kamato, D., Burch, M. L., Piva, T. J., Rezaei, H. B., Rostam, M. A., Xu, S., ... Osman, N. (2013). Transforming growth factor-beta signalling: Role and consequences of Smad linker region phosphorylation. *Cellular Signalling*, 25(10), 2017–2024. <https://doi.org/10.1016/j.cellsig.2013.06.001>
- Kim, I. Y., Ahn, H. J., Zelner, D. J., Shaw, J. W., Sensibar, J. A., Kim, J. H., ... Lee, C. (1996). Genetic change in transforming growth factor beta (TGF-beta) receptor type I gene correlates with insensitivity to TGF-beta 1 in human prostate cancer cells. *Cancer Research*, 56(1), 44–48.
- Kim, I. Y., Zelner, D. J., Sensibar, J. A., Ahn, H. J., Park, L., Kim, J. H., & Lee, C. (1996). Modulation of sensitivity to transforming growth factor-beta 1 (TGF-beta 1) and the level of type II TGF-beta receptor in LNCaP cells by dihydrotestosterone. *Experimental Cell Research*, 222(1), 103–110. <https://doi.org/10.1006/excr.1996.0013>
- Kim, J., Kong, J., Chang, H., Kim, H., & Kim, A. (2016). EGF induces epithelial-mesenchymal transition through phospho-Smad2/3-snail signaling pathway in breast cancer cells. *Oncotarget*, 7(51), 85021–85032. <https://doi.org/10.18632/oncotarget.13116>
- Kim, J. H., Lee, C. H., & Lee, S. W. (2016). Hepatitis C virus infection stimulates transforming growth factor-beta1 expression through up-regulating miR-192. *Journal of Microbiology*, 54(7), 520–526. <https://doi.org/10.1007/s12275-016-6240-3>
- Kindrachuk, J., Wahl-Jensen, V., Safronetz, D., Trost, B., Hoenen, T., Arsenault, R., ... Jahrling, P. B. (2014). Ebola virus modulates transforming growth factor beta signaling and cellular markers of mesenchyme-like transition in hepatocytes. *Journal of Virology*, 88(17), 9877–9892. <https://doi.org/10.1128/JVI.01410-14>
- Kwaan, H. C., Wang, J., Svoboda, K., & Declerck, P. J. (2000). Plasminogen activator inhibitor 1 may promote tumour growth through inhibition of apoptosis. *British Journal of Cancer*, 82(10), 1702–1708. <https://doi.org/10.1054/bjoc.2000.1207>
- Lamouille, S., Xu, J., & Derynck, R. (2014). Molecular mechanisms of epithelial-mesenchymal transition. *Nature Reviews. Molecular Cell Biology*, 15(3), 178–196. <https://doi.org/10.1038/nrm3758>
- Law, M., Carter, G. C., Roberts, K. L., Hollinshead, M., & Smith, G. L. (2006). Ligand-induced and nonfusogenic dissolution of a viral membrane. *Proceedings of the National Academy of Sciences of the United States of America*, 103(15), 5989–5994. <https://doi.org/10.1073/pnas.0601025103>
- Leite, F. G. G., Torres, A. A., De Oliveira, L. C., Da Cruz, A. F. P., Soares-Martins, J. A. P., Pereira, A., ... Bonjardim, C. A. (2017). C-Jun integrates signals from both MEK/ERK and MKK/JNK pathways upon vaccinia virus infection. *Archives of Virology*, 162(10), 2971–2981. <https://doi.org/10.1007/s00705-017-3446-6>
- Levy, L., & Hill, C. S. (2005). Smad4 dependency defines two classes of transforming growth factor [beta] (TGF-[beta]) target genes and distinguishes TGF-[beta]-induced epithelial-mesenchymal transition from its antiproliferative and migratory responses. *Molecular and Cellular Biology*, 25(18), 8108–8125. <https://doi.org/10.1128/MCB.25.18.8108-8125.2005>
- Levy, L., Howell, M., Das, D., Harkin, S., Episkopou, V., & Hill, C. S. (2007). Arkadia activates Smad3/Smad4-dependent transcription by triggering signal-induced SnoN degradation. *Molecular and Cellular Biology*, 27(17), 6068–6083. <https://doi.org/10.1128/mcb.00664-07>
- Li, F., Goncalves, J., Faughnan, K., Steiner, M. G., Pagan-Charry, I., Esposito, D., ... Staiano-Coico, L. (2000). Targeted inhibition of wound-induced PAI-1 expression alters migration and differentiation in human epidermal keratinocytes. *Experimental Cell Research*, 258(2), 245–253. <https://doi.org/10.1006/excr.2000.4918>
- Liu, L., Cooper, T., Howley, P. M., & Hayball, J. D. (2014). From crescent to mature virion: Vaccinia virus assembly and maturation. *Viruses*, 6(10), 3787–3808. <https://doi.org/10.3390/v6103787>
- Lynn, H., Horsington, J., Ter, L. K., Han, S., Chew, Y. L., Diefenbach, R. J., ... Newsome, T. P. (2012). Loss of cytoskeletal transport during egress critically attenuates ectromelia virus infection in vivo. *Journal of Virology*, 86(13), 7427–7443. <https://doi.org/10.1128/JVI.06636-11>
- Macias, M. J., Martin-Malpartida, P., & Massague, J. (2015). Structural determinants of Smad function in TGF-beta signaling. *Trends in Biochemical Sciences*, 40(6), 296–308. <https://doi.org/10.1016/j.tibs.2015.03.012>
- Maluquer de Motes, C., & Smith, G. L. (2017). Vaccinia virus protein A49 activates Wnt signalling by targeting the E3 ligase beta-TrCP. *The Journal of General Virology*, 98, 3086–3092. <https://doi.org/10.1099/jgv.0.000946>

- Marzook, N. B., Latham, S. L., Lynn, H., McKenzie, C., Chaponnier, C., Grau, G. E., & Newsome, T. P. (2017). Divergent roles of beta- and gamma-Actin isoforms during spread of vaccinia virus. *Cytoskeleton (Hoboken)*, 74(4), 170–183. <https://doi.org/10.1002/cm.21356>
- Meindl-Beinker, N. M., Matsuzaki, K., & Dooley, S. (2012). TGF-beta signaling in onset and progression of hepatocellular carcinoma. *Digestive Diseases*, 30(5), 514–523. <https://doi.org/10.1159/000341704>
- Mercer, J., & Helenius, A. (2008). Vaccinia virus uses macropinocytosis and apoptotic mimicry to enter host cells. *Science*, 320(5875), 531–535. <https://doi.org/10.1126/science.1155164>
- Moss, B. (1968). Inhibition of HeLa cell protein synthesis by the vaccinia virion. *Journal of Virology*, 2(10), 1028–1037.
- Parrish, S., Resch, W., & Moss, B. (2007). Vaccinia virus D10 protein has mRNA decapping activity, providing a mechanism for control of host and viral gene expression. *Proceedings of the National Academy of Sciences of the United States of America*, 104(7), 2139–2144. <https://doi.org/10.1073/pnas.0611685104>
- Pereira, A. C., Leite, F. G., Brasil, B. S., Soares-Martins, J. A., Torres, A. A., Pimenta, P. F., ... Bonjardim, C. A. (2012). A vaccinia virus-driven interplay between the MKK4/7-JNK1/2 pathway and cytoskeleton reorganization. *Journal of Virology*, 86(1), 172–184. <https://doi.org/10.1128/JVI.05638-11>
- Peters, N. E., Ferguson, B. J., Mazzon, M., Fahy, A. S., Krysztowska, E., Arribas-Bosacoma, R., ... Smith, G. L. (2013). A mechanism for the inhibition of DNA-PK-mediated DNA sensing by a virus. *PLoS Pathogens*, 9(10), e1003649. <https://doi.org/10.1371/journal.ppat.1003649>
- Potts, K. G., Irwin, C. R., Favis, N. A., Pink, D. B., Vincent, K. M., Lewis, J. D., ... Evans, D. H. (2017). Deletion of F4L (ribonucleotide reductase) in vaccinia virus produces a selective oncolytic virus and promotes anti-tumor immunity with superior safety in bladder cancer models. *EMBO Molecular Medicine*, 9(5), 638–654. <https://doi.org/10.15252/emmm.201607296>
- Providence, K. M., & Higgins, P. J. (2004). PAI-1 expression is required for epithelial cell migration in two distinct phases of in vitro wound repair. *Journal of Cellular Physiology*, 200(2), 297–308. <https://doi.org/10.1002/jcp.20016>
- Ran, F. A., Hsu, P. D., Wright, J., Agarwala, V., Scott, D. A., & Zhang, F. (2013). Genome engineering using the CRISPR-Cas9 system. *Nature Protocols*, 8(11), 2281–2308. <https://doi.org/10.1038/nprot.2013.143>
- Rice, A. P., & Roberts, B. E. (1983). Vaccinia virus induces cellular mRNA degradation. *Journal of Virology*, 47(3), 529–539.
- Rostam, M. A., Kamato, D., Piva, T. J., Zheng, W., Little, P. J., & Osman, N. (2016). The role of specific Smad linker region phosphorylation in TGF-beta mediated expression of glycosaminoglycan synthesizing enzymes in vascular smooth muscle. *Cellular Signalling*, 28(8), 956–966. <https://doi.org/10.1016/j.cellsig.2016.05.002>
- Rottger, S., Frischknecht, F., Reckmann, I., Smith, G. L., & Way, M. (1999). Interactions between vaccinia virus IEV membrane proteins and their roles in IEV assembly and Actin tail formation. *Journal of Virology*, 73(4), 2863–2875.
- Rowan, A. G., Fletcher, J. M., Ryan, E. J., Moran, B., Hegarty, J. E., O'Farrelly, C., & Mills, K. H. (2008). Hepatitis C virus-specific Th17 cells are suppressed by virus-induced TGF-beta. *Journal of Immunology*, 181(7), 4485–4494.
- Rubins, K. H., Hensley, L. E., Relman, D. A., & Brown, P. O. (2011). Stunned silence: Gene expression programs in human cells infected with monkeypox or vaccinia virus. *PLoS One*, 6(1), e15615. <https://doi.org/10.1371/journal.pone.0015615>
- Sanderson, C. M., Way, M., & Smith, G. L. (1998). Virus-induced cell motility. *Journal of Virology*, 72(2), 1235–1243.
- Sattentau, Q. (2008). Avoiding the void: Cell-to-cell spread of human viruses. *Nature Reviews. Microbiology*, 6(11), 815–826. <https://doi.org/10.1038/nrmicro1972>
- Schmidt, F. I., Bleck, C. K., Helenius, A., & Mercer, J. (2011). Vaccinia extracellular virions enter cells by macropinocytosis and acid-activated membrane rupture. *The EMBO Journal*, 30(17), 3647–3661. <https://doi.org/10.1038/emboj.2011.245>
- Schmidt, F. I., Bleck, C. K., Reh, L., Novy, K., Wollscheid, B., Helenius, A., ... Mercer, J. (2013). Vaccinia virus entry is followed by core activation and proteasome-mediated release of the immunomodulatory effector VH1 from lateral bodies. *Cell Reports*, 4(3), 464–476. <https://doi.org/10.1016/j.celrep.2013.06.028>
- Shaulian, E. (2010). AP-1—the Jun proteins: Oncogenes or tumor suppressors in disguise? *Cellular Signalling*, 22(6), 894–899. <https://doi.org/10.1016/j.cellsig.2009.12.008>
- Souchelnytskyi, S., Tamaki, K., Engstrom, U., Wernstedt, C., ten Dijke, P., & Heldin, C. H. (1997). Phosphorylation of Ser465 and Ser467 in the C terminus of Smad2 mediates interaction with Smad4 and is required for transforming growth factor-beta signaling. *The Journal of Biological Chemistry*, 272(44), 28107–28115.
- Stanifer, M. L., Rippert, A., Kazakov, A., Willemsen, J., Bucher, D., Bender, S., ... Boulant, S. (2016). Reovirus intermediate subviral particles constitute a strategy to infect intestinal epithelial cells by exploiting TGF-beta dependent pro-survival signaling. *Cellular Microbiology*, 18(12), 1831–1845. <https://doi.org/10.1111/cmi.12626>
- Strnadova, P., Ren, H., Valentine, R., Mazzon, M., Sweeney, T. R., Brierley, I., & Smith, G. L. (2015). Inhibition of translation initiation by protein 169: A vaccinia virus strategy to suppress innate and adaptive immunity and Alter virus virulence. *PLoS Pathogens*, 11(9), e1005151. <https://doi.org/10.1371/journal.ppat.1005151>
- Stuart, J. H., Sumner, R. P., Lu, Y., Snowden, J. S., & Smith, G. L. (2016). Vaccinia virus protein C6 inhibits type I IFN Signalling in the nucleus and binds to the transactivation domain of STAT2. *PLoS Pathogens*, 12(12), e1005955. <https://doi.org/10.1371/journal.ppat.1005955>
- Teicher, B. A. (2001). Malignant cells, directors of the malignant process: Role of transforming growth factor-beta. *Cancer Metastasis Reviews*, 20(1–2), 133–143.
- Twardzik, D. R., Brown, J. P., Ranchalis, J. E., Todaro, G. J., & Moss, B. (1985). Vaccinia virus-infected cells release a novel polypeptide functionally related to transforming and epidermal growth factors. *Proceedings of the National Academy of Sciences of the United States of America*, 82(16), 5300–5304.
- Valderrama, F., Cordeiro, J. V., Schleich, S., Frischknecht, F., & Way, M. (2006). Vaccinia virus-induced cell motility requires F11L-mediated inhibition of RhoA signaling. *Science*, 311(5759), 377–381. <https://doi.org/10.1126/science.1122411>
- Vo, B. T., Morton, D., Jr., Komaragiri, S., Millena, A. C., Leath, C., & Khan, S. A. (2013). TGF-beta effects on prostate cancer cell migration and invasion are mediated by PGE2 through activation of PI3K/AKT/mTOR pathway. *Endocrinology*, 154(5), 1768–1779. <https://doi.org/10.1210/en.2012-2074>
- Wang, Y., Shi, J., Chai, K., Ying, X., & Zhou, B. P. (2013). The role of snail in EMT and tumorigenesis. *Current Cancer Drug Targets*, 13(9), 963–972.
- Wilding, G., Zugmeier, G., Knabbe, C., Flanders, K., & Gelmann, E. (1989). Differential effects of transforming growth factor beta on human prostate cancer cells in vitro. *Molecular and Cellular Endocrinology*, 62(1), 79–87.
- Wrighton, K. H., Lin, X., & Feng, X. H. (2009). Phospho-control of TGF-beta superfamily signaling. *Cell Research*, 19(1), 8–20. <https://doi.org/10.1038/cr.2008.327>
- Xu, J., Lamouille, S., & Derynck, R. (2009). TGF-beta-induced epithelial to mesenchymal transition. *Cell Research*, 19(2), 156–172. <https://doi.org/10.1038/cr.2009.5>
- Yang, J., Tian, B., Sun, H., Garofalo, R. P., & Brasier, A. R. (2017). Epigenetic silencing of IRF1 dysregulates type III interferon responses to respiratory virus infection in epithelial to mesenchymal transition. *Nature Microbiology*, 2, 17086. <https://doi.org/10.1038/nmicrobiol.2017.86>

- Yoo, Y. D., Ueda, H., Park, K., Flanders, K. C., Lee, Y. I., Jay, G., & Kim, S. J. (1996). Regulation of transforming growth factor-beta 1 expression by the hepatitis B virus (HBV) X transactivator. Role in HBV pathogenesis. *The Journal of Clinical Investigation*, 97(2), 388–395. <https://doi.org/10.1172/JCI118427>
- Yook, J. I., Li, X. Y., Ota, I., Fearon, E. R., & Weiss, S. J. (2005). Wnt-dependent regulation of the E-cadherin repressor snail. *The Journal of Biological Chemistry*, 280(12), 11740–11748. <https://doi.org/10.1074/jbc.M413878200>
- Zhang, Y., Feng, X. H., & Derynck, R. (1998). Smad3 and Smad4 cooperate with c-Jun/c-Fos to mediate TGF-beta-induced transcription. *Nature*, 394(6696), 909–913. <https://doi.org/10.1038/29814>
- Zhao, X., Nicholls, J. M., & Chen, Y. G. (2008). Severe acute respiratory syndrome-associated coronavirus nucleocapsid protein interacts with Smad3 and modulates transforming growth factor-beta signaling. *The Journal of Biological Chemistry*, 283(6), 3272–3280. <https://doi.org/10.1074/jbc.M708033200>
- Zhu, S., Wang, W., Clarke, D. C., & Liu, X. (2007). Activation of Mps1 promotes transforming growth factor-beta-independent Smad signaling. *The Journal of Biological Chemistry*, 282(25), 18327–18338. <https://doi.org/10.1074/jbc.M700636200>

SUPPORTING INFORMATION

Additional supporting information may be found online in the Supporting Information section at the end of this article.

How to cite this article: Gowripalan A, Abbott CR, McKenzie C, et al. Cell-to-cell spread of vaccinia virus is promoted by TGF- β -independent Smad4 signalling. *Cellular Microbiology*. 2020;22:e13206. <https://doi.org/10.1111/cmi.13206>